UNIVERSITETET I AGDER

Theoretical and Experimental Study of Novel Types of Solid Oxide Fuel Cell Electrodes

SASANKA NIROMI RANASINGHE

SUPERVISOR
Professor Peter Hugh Middleton

University of Agder, [2017]
Faculty of Engineering and Science
Department of Engineering Sciences

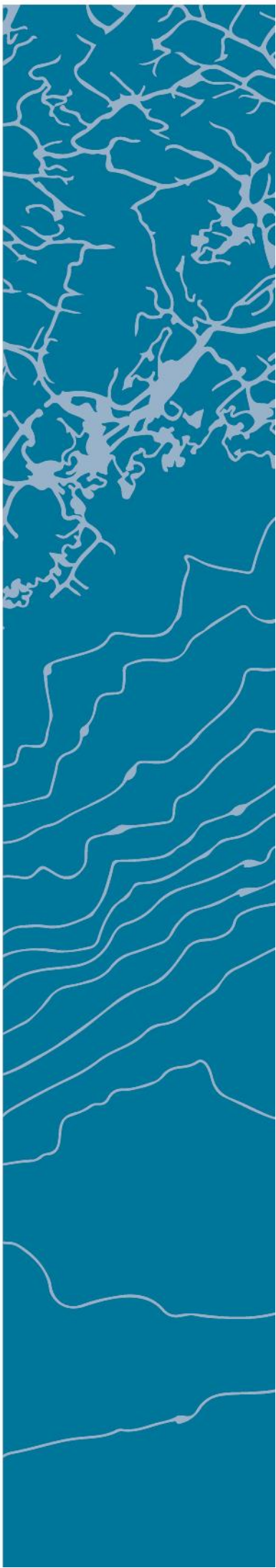

Abstract

Solid oxide fuel cells (SOFCs) have the potential to become one of the efficient and cost-effective system for direct conversion of a wide variety of fuels to electricity. The performance, stability and durability of SOFCs depend strongly on the materials used for the fabrication of electrodes as well as the fabrication process. For anode supported SOFCs, the tape casting method has been the *de facto* standard for constructing cell components. Furthermore, organic solvents such as ethanol, propanol, terpineol and poly-ethers are generally used in industrial tape casting as the solvent medium to make the chemical slurries out of ceramic powders. Although, the use of organic solvents makes the dispersion of solid chemical particles relatively easier, it is not an environmentally friendly solution.

In this thesis, we address this issue by investigating the possibility of fabricating anode supported SOFC cell components using water instead organic solvents. In addition, this thesis also looks at other aspects of fabricating anode supported cells, namely the need for active and barrier layers to prevent undesirable side relations during sintering and also to improve the performance of the fuel cell. We have in particular looked at the variation in the porosity of the anode support layer and the use of active layers and barrier layers. Hence, the fabricated SOFCs have five layers, namely the anode, active, electrolyte, barrier and the cathode layers.

In order to validate the performance characteristics of the fabricated SOFCs, we have also modelled equivalent theoretical models using COMSOL Multiphysics (version 5.2) software. Our theoretical models are 3D models that are well suited to developing better approximations to the actual experimental data.

The experimental performance was comparable to expectations based on literature data and indicated that our water based formulations are suitable for SOFC development. Moreover, our COMSOL model was able to fit the experimental behavior with careful selection of parameters.

Keywords: *Solid oxide fuel cells, fabrication, modelling, simulation.*

Preface

This report serves as a Master's Thesis in Solid Oxide Fuel Cells (SOFCs) to fulfill the requirements of the Master's Program in Renewable Energy at the Faculty of Engineering and Science, University of Agder (UiA) in Grimstad, Norway. The research was started on 1st August 2016 and ended on 30th January 2017. The main objective of this thesis is the evaluation of the performance of single cell SOFCs having electrodes with a different chemical compositions.

I am delighted to take this opportunity to show my sincere gratitude to all the ones who have helped me in achieving our goals. I am greatly obliged to my supervisor, Professor Peter Hugh Middleton for his valuable assistance in giving feedback on project work throughout the semester. I am also grateful to Mr.Raphael Ihringer, Mr.Andre Pappas and Mr.Pierre Coquoz who are the members of Fiaxell lab in EPFL, Lausanne, Switzerland for their valuable guidance and giving me the opportunity to get hands-on experience in fabricating and testing of SOFCs.

I am also grateful to my husband G. P. Harsha Sandaruwan, who is a Doctoral Fellow in the department of ICT and Dr. Indika Anuradha Mendis for their valuable thoughts and guidance. It is my duty to also thank Jagath Sri Lal Senanayake who is a Doctoral Fellow in the department of Mechatronics for helping me to get familiarized with the basics of the COMSOL Multiphysics software.

Last, but certainly not the least, I would like to express my gratefulness and humility to my parents, brothers and friends for their support during the Master's Thesis.

Grimstad
January, 2017
S.N.Ranasinghe

Contents

List of Figures

List of Tables

Abbreviations

AFC	Alkaline Fuel Cell
ASC	Anode Supported Cell
C	Carbon
CeO_2	Cerium Dioxide
CFD	Computational Fluid Dynamics
CH_4	Methane
CO	Carbon Monoxide
CO_2	Carbon Dioxide
e	Electron
EMF	Electromotive Force
ESC	Electrolyte Supported Cell
Gd_2O_3	Gadolinium (III) Oxide
GDC	Gadonium doped Ceria
GDE	Gas Diffusion Electrode
H^+	Ionized Hydrogen
H_2	Hydrogen
$LSCF$	Lanthanum Strontium Cobalt Ferrite
LSM	Strontium-doped Lanthanum Manganite
$LTNE$	Local Temperature Non-Equilibrium
$MCFC$	Molten Carbonate Fuel Cell
N_2	Nitrogen
NiO_2	Nickel Oxide
O^{2-}	Ionized Oxygen
O_2	Oxygen

OCV	Open Circuit Voltage
$PAFC$	Phosphoric Acid Fuel Cell
PEM	Proton Exchange Membrane
Pt	Platinum
$SCFC$	Single-chamber Fuel Cell
$SOFC$	Solid Oxide Fuel Cell
$SrZrO_3$	Strontium Zirconate
YSZ	Yttria-Stabilized Zirconia
ZrO_2	Zirconium Dioxide

Chapter 1

Introduction

In this chapter, we provide background information on fuel cells including how they operate along with a brief comparison between the different fuel cell types. Then, we have stated our contribution and scope of work, research objectives followed by a literature review in the area of our interest. Finally, an outline describing the structure of the upcoming chapters are provided.

1.1 Fuel Cell Basics

A fuel cell is a device which is capable of converting chemical energy obtained from fuel into electrical energy. It produces energy without having any form of combustion while releasing fewer pollutants (water and heat) to the environment. Hence, fuel cells are environmental friendly devices utilized for power generation via energy conversion. However, the development of fuel cells and the usage of fuel cells for practical applications are not yet widely developed like other energy conversion technologies such as bio-gas, photovoltaic and wind energy [8]. The reason is primarily due to the cost of production and the lack of infrastructure to supply pure Hydrogen (H_2) as a fuel. The work described in this thesis is focussed on one particular type of fuel cell, namely the Solid Oxide Fuel Cell (SOFC) which operates at a high temperature around $800°C$.

Fuel cells operate like a battery. However, a battery generates electricity with reactions of chemicals inside the battery while fuel cells are capable of generating an electromotive force (EMF) continuously, when the required inputs (fuel and oxidants) fed externally. Fuel cells are mostly used in transportation, stationary power generation and battery replacement. In transport applications, it is common to use a fuel cell battery hybrid which combines the best features of both fuel cells and batteries to give optimum performance.

A fuel cell consists of three main parts, anode, cathode and an electrolyte, which is sandwiched between the anode and the cathode. The operation of the fuel cell is as follows. In the anode, externally supplied H_2 reacts on the catalyst creating ionized Hydrogen (H^+) and electrons (e). These electrons passing through the external circuit producing an electrical

Table 1.1: Comparison of Different Types of Fuel Cells

Fuel Cell Type	AFC	PEM	MCFC	PAFC	SOFC
Common Electrolyte	Potassium hydroxide	Ion exchange membrane	Immobilized liquid molten carbonate	Immobilized liquid phosphoric acid	Ceramic
Operating Temperature	$90°C - 100°C$	$50°C - 100°C$	$600°C - 700°C$	$150°C - 200°C$	$700°C - 1000°C$
Efficiency	60%	For transportation - 60%	45%-50%	40%	60%
Electrical Power	Up to $20kW$	Up to $250kW$	$> 1MW$	$> 50kW$	$> 200kW$
Applications	Military, Space	Transportation, Distributed generation	Distributed generation, Military applications	Stationary power generation	Auxiliary power, Distributed generation
Advantages	High performance, Can use non-precious metals catalysts (nitrogen doped-carbon)	Compact construction, Solid electrolyte, low working temperature	High efficiency, Low cost	Can use impure H_2 as fuel, Less pollution	No electrode corrosion, No need of expensive catalysts (Platinum), Less pollution
Disadvantages	Increased corrosion, Difficult to handle in differential pressure, CO_2 poisoning	Water management, CO sensitive, Cooling issues	Low durability, Affect to high temperature corrosion	Low efficiency, Low power density, Expensive	Need thermally stable materials, Complex fabrication

current while H^+ passes through the electrolyte. In the case of SOFCs, Oxygen ions (O^{2-}) are the conducting species within the solid electrolyte. In the cathode, Oxygen (O_2) from air reacts with H^+ and electrons forming water and heat. The general overview of the operation (inputs and outputs) of a fuel cell is shown in Figure 1.1. In the case of the SOFC, the product water is directly produced on the anode.

Figure 1.1: General overview of operation of fuel cell

There are many types of fuel cells such as Alkaline Fuel Cell (AFC), Proton Exchange Membrane (PEM) Fuel Cell, Molten Carbonate Fuel Cell (MCFC), Phosphoric Acid Fuel Cell (PAFC) and Solid Oxide Fuel Cell (SOFC). A comparison of the aforementioned fuel cell types are tabulated in Table 1.1.

1.2 Solid Oxide Fuel Cell (SOFC)

In general, SOFCs have high electrical efficiency and relatively low cost compared to other types of fuel cells such as AFC, PEM and PAFC. Given that, they were originally conceived to use coal as the fuel, they were referred as *Coal gas cells*. Nowadays, both natural gasses and coal-derived gasses are used as the primary sources of fuel for SOFCs. SOFCs do not use any kind of liquid for their operation. Therefore, SOFCs are also known as two phase interface cells (gas-solid) and this property helps in increasing the cell performance as well as the lifetime. Usually, SOFCs use electrolytes fabricated with Yttria-Stabilized Zirconia (YSZ) while Nickel Oxide (NiO_2) and Strontium-doped Lanthanum Manganite (LSM) are used for the construction of anodes and cathodes respectively.

The operation of a SOFC is graphically shown in Figure 1.2. O_2 from air reacts with the cathode and produce O^{2-} in the cathode. These ions pass through the electrolyte to the anode. In the anode, H_2 reacts with O^{2-} and produces water and electrons [9] [10].

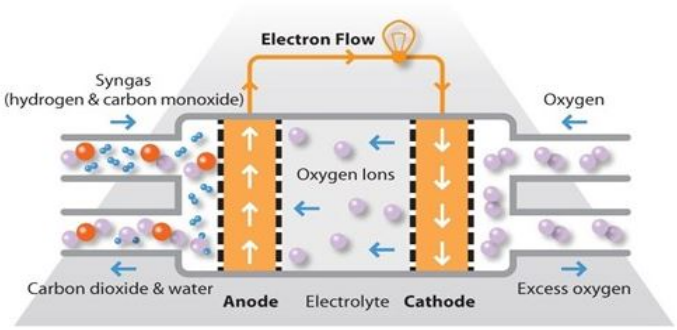

Figure 1.2: Operation of SOFC [1]

The governing equations for anode and cathode reactions are stated below.

$$Anode\ reaction: \quad 2H_2 + 2O_2 \rightleftharpoons 2H_2O + 4e \tag{1.1}$$

$$Cathode\ reaction: \quad O_2 + 4e \rightleftharpoons 2O_2^- \tag{1.2}$$

In the simplest mode of operation, SOFCs use pure H_2 as the fuel for their operation as shown in Equation 1.1. However, given that SOFCs operate on higher temperatures ($800°C - 1000°C$), it is possible to use other gasses such as Methane (CH_4) and produce H_2 internally, with the help of a metal catalyst. Hence, the practical difficulty of externally feeding pure H_2 can be eliminated. In this respect, we used the term *fuel flexibility*. The reactions associated with the aforementioned steam reforming process are:

$$CH_4 + H_2O + catalyst \rightarrow 3H_2 + CO \tag{1.3}$$

$$CO + H_2O \rightleftharpoons 2H_2 + CO_2 \tag{1.4}$$

As a result of the above two reactions, both Carbon Monoxide (CO) and Carbon Dioxide (CO_2) are present in the system itself. Then the Boudouard reaction,

$$C + CO_2 \rightleftharpoons 2CO \tag{1.5}$$

occurs and it produces Carbon (C) in the form of a fine solid called *soot* in the system. The soot will accumulate on the anode, creating a Carbon deposit on the anode surface affecting the efficiency of the cell. However, when the operating temperature is greater than $600°C$, the Equation 1.5 triggers towards the forward direction which ultimately helps in eliminating the accumulation of excessive Carbon in the anode. In practice, excess water in the form of steam is added to the input to avoid Carbon deposition.

The simpler concept, design and construction, higher efficiency, fuel flexibility and relatively high power density are some of the advantages of SOFCs.

1.3 Solid Oxide Fuel Cell Structure

There are two types of SOFCs based on the geometry, planar SOFCs and tubular SOFCs. The planar SOFCs are the most general version, fabricated as a stack of thin layers. On the other hand, tubular cells consist of long cathode tubes where the anode and the electrolyte are laminated and operates in $900°C$ - $1000°C$ [11] [12]. Short current paths resulting in low electrical resistance, high power densities and easier fabrication make planar SOFCs more reliable. However, problems in sealing and interconnections are the main drawbacks for these types of SOFCs. In comparison to planar SOFCs, tubular SOFCs have higher electrical resistance.

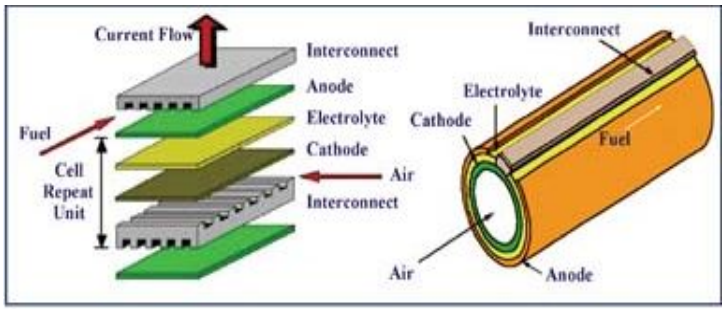

Figure 1.3: Planar and tubular SOFC [2]

SOFCs can be further divided into two types as anode supported cells (ASC) and electrolyte supported cells (ESC) based on their fabrication as shown in Figure 1.4. The anode is acting as the base of ASCs while the electrolyte is acting as the base of the ESCs [13] [14]. The main advantage of ASCs compared to ESCs is that the thin electrolyte in ASCs provides lower resistance which helps in improving the performance of the cell.

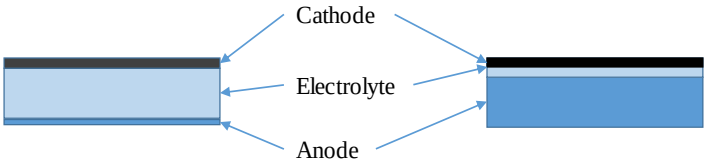

Figure 1.4: Electrolyte supported cell and anode supported cell

1.4 Contribution and Scope of Work

This Masters thesis focuses on the development of tape casting formulas for making SOFC cells based on ASC concepts.

In the past, tape casting has been widely used to make SOFC components and has become a de facto standard for making ASC types of cells. The method is highly suitable for mass production and is relatively cost effective. However, most formulas use organic based solvents and "vehicles" that present an environmental hazard and are not so easily recycled. In this work, we have prepared water based systems that minimize these types of hazards and present a more environmentally friendly solution. Similar methods have also been applied in this work to making water based screen printing inks that otherwise almost always use organic solvents.

One of the main reasons that organic solvents such as ethanol, propanol, terpineol and poly-ethers are used is that they have very desirable surface tension properties that make dispersion of solid ceramic particles relatively easy which allows the "paint" or "ink" to adhere to the substrate without "crawling" or forming droplets. Given that the tapes are made in a continuous process in a manufacturing context, stability of the cast tape (and screen printed layer) is essential.

Another aspect is that the use of a water base also avoids the need to have very precise humidity control. This is a major problem with organic based formulas that can suffer from "skinover" or non-uniform shrinkage, if the water level in the atmosphere is either too low or too high. In the case of water based systems, this is completely eliminated thus allowing the tape layers to dry naturally and fast using forced air dryers. This then allows for much faster rates of production and simplified quality control - all leading to cost reduction. Moreover, the minimization of hazardous solvent vapours from the production lab means that personnel do not need to wear protective breathing apparatus or labs with fume extraction.

This thesis also looks at other essential aspects of fabricating ASCs, namely the need for active and barrier layers to prevent undesirable side relations during sintering and also to improve the performance of the fuel cell. We have in particular looked at the variation in the porosity of the anode support layer and the use of active layers and barrier layers.

To complete the Maters level study, we have also carried out some modelling work to allow comparison with the experimental data and to increase our understanding of the functionally of the cell testing set up. For this purpose, we have adapted a finite element analysis approach using COMSOL Multiphysics software (version 5.2).

1.5 Research Objectives

SOFCs operate at higher temperatures than other types of fuel cells. Therefore, SOFCs need thermally stable materials as the electrodes. As stated in Table 1.1, the efficiency of an SOFC is approximately about 60% [1]. Thus, there is a need for identifying appropriate mechanisms to improve the performance of SOFCs. We have summarized the main thesis objectives that are intended to be addressed during this Masters thesis.

- Fabricate SOFC single cells using ASC concepts and replacing conventional organic solvents with a water base to make an all aqueous ceramic tape casting slurry (paste).
- Fabricate two formulations of the anode support with different sizes of NiO_2 particles with the intention of varying and improving performance.
- Perform experiments to observe the characteristics (polarization characteristics and power characteristics) of the fabricated SOFC cells.
- Develop theoretical models equivalent to the fabricated SOFCs using COMSOL software and obtain the cell characteristics of the modelled SOFCs.
- Compare the theoretical and experimental results to validate the experimental cell characteristics.

1.6 Brief Review of Related Work

This section provides the related work regarding the theoretical and experimental analysis of SOFCs. We have provided the related research works regarding fabrication of SOFCs followed by the research work regarding the theoretical modelling of SOFCs.

1.6.1 SOFC Fabrication

Rotureau D. et al. [15] investigated the capability of using screen printing technology to manufacture planar SOFCs. They have used widely studied materials of YSZ for the electrolyte, LSM for the cathode and $Ni-YSZ$ ($Ni\,and\,YSZ$) for the anode. Two types of SOFCs have been considered in their study. First type is called as the conventional two-chamber device, where the fuel is supplied separately for the anode and the cathode. The second type was called as the single-chamber fuel cells (SCFC), where both the anode and the cathode are put in the same side of the electrolyte to have a common atmosphere. In order to evaluate the performance, two test benches were used for the two test cases mentioned above. The main drawbacks of their fabrication are that, they use a gold current collector with Platinum (Pt) layer as a catalyst which increase the cost of the cell as well as the use of $Ni-YSZ$ for the anode which affects the performance.

Stover D. et al. [16] have conducted a research based on the processing methods, properties and alternative materials for the fabrication of multilayer SOFCs. The chemicals used for the fabrication of SOFCs are same as in [15]. As processing methods of the SOFCs, they considered warm-pressing (where the powders are coated with a binder and pressed), tape casting method, vacuum-slip-casting and wet powder spraying (similar to screen printing) for their analysis. Furthermore, they have considered tubular and planar SOFCs. By comparing the processing methods mentioned above, the have concluded that it is better to use the tape casting or screen printing process for electrode fabrication, which is the cheapest option. Given that they used the same materials for the fabrication as in [15], the same drawbacks in [15] are valid to [16] as well.

In Mahata et al [17], details of a tubular SOFC having the anode and the electrolyte fabricated with co-pressing in cold iso-static press (CIP) is presented. Furthermore, the dip-coating technique was used to fabricate the cathode and the cathode current collector. Moreover, co-firing technique (at $1350°C$) was used to sinter the anode and the electrolyte. They have used organic solvents for making the slurries for all the electrodes. High wire resistance, lack of sealing led to the poor performance of their fabricated cells.

Kim K.J et al [18] suggested a method to fabricate an intermediate temperature SOFC using tape casting and co-sintering processes. They have used $LSGM8282$ ($La_{0.8}Sr_{0.2}Ga_{0.8}Mg_{0.2}O_{3-8}$) material to fabricate a thin electrolyte. A buffer layer (LDC) and the anode layer (consisted with Ni/GDC) complete the SOFC. The performance can be further improved by reducing the thickness of the electrolyte (which was 40 μm).

Beltran-Lopez J.F et al. [19], proposed a method to construct graded anodes for SOFCs using tape casting and cold lamination plates of different compositions. They have adjusted the Rheological parameters to obtain a stable suspension for the tape casting process. Furthermore, they have laminated the plates at room temperature without using plasticisers by introducing two binders which undergo plastic deformation at room temperature. Porosity and resistivity measurements are used to evaluate the performance of this method. Finally, they have concluded that fabricating graded anodes for SOFCs using this method is cost effective and versatile.

In this thesis, we have used the tape casting and screen printing processes for fabricating the electrodes of the SOFCs. Furthermore, we have used $NiO_2 - YSZ$ as the anode material (instead of using $Ni - YSZ$ as was in [15, 16]), and YSZ as the electrolyte material to investigate whether it will provide a superior performance.

1.6.2 SOFC Modelling

This subsection provides the related work regarding modelling of SOFCs. Laksmi T.V.V.S. et al. [20], proposed a method to evaluate the performance of a single cell SOFC with the help of a MATLAB/Simulink theoretical model. They have developed a model to obtain the steady state characteristics. They have considered two different operating temperatures ($800°C$ and

$850°C$) as well as four different flow rates (31 ml/sec, 36 ml/sec, 41 ml/sec and 51 ml/sec) for the simulations. In order to obtain better performance activation loss, concentration loss and ohmic loss were considered in the model. Finally, the simulation results were used to validate their experimental results provided in [21].

Gebregergis A. et al. [21] proposed a method to analyze the dynamic response of a SOFC by introducing the distributed modelling approach and lumped modelling. They have used the lumped model which can be extended to a fuel cell stack and used it to the computation of real-time control. In developing the lumped model, the basic electrochemical equations were used. Furthermore, the partial pressures of gases were used as the exit pressures for the model and this model was developed by using the PSpice software. The distributed model was used to obtain the experimental results. They have considered the anode supported counter-flow tubular cell design and assumed that the partial pressures of O_2, H_2 and water vary throughout the length of the fuel cell. In this paper, they have also provided the I-V curves for different flow rates as in [20], the polarization curves for different temperatures and the dynamic response of the cell. It is observable that both models have similar time responses and the response time does not change significantly with the SOFC temperature.

A computational fluid dynamics (CFD) 2D model for SOFC unit cell is modelled using COMSOL Multiphyiscs (version 3.5) for an anode supported intermediate temperature SOFC in [22]. Authors have considered equations for heat, mass and momentum transport for the model. Furthermore, a local temperature non-equilibrium (LTNE) approach is used to calculate the temperature distribution in both gas and solid phases of the model. They have also extended the aforementioned basic model to investigate the effect of internal reforming reactions of SOFCs. The main findings of their study is that, the activation polarization in the anode and the cathode and the ohmic polarization of the electrolyte have major influence on the efficiency.

Paradis H. [23] developed a CFD model by using COMSOL Multiphysics (version 3.5a) software as an extension of [22] by introducing different internal reforming reactions. Both [22] and [23] considered 2D models for their analysis. Furthermore, [23] compared the obtained results with two different models in terms of reaction rates and effects of the transport processes.

In our thesis, we have used the COMSOL Multiphysics software (version 5.2) to develop the equivalent theoretical models for the fabricated SOFCs to validate the characteristics obtained by carrying out the experiments on the fabricated SOFCs. We have used the COMSOL models for our theoretical simulations, given that the COMSOL models provide a superior approximation to experimental scenarios than MATLAB simulation models. However, there are no any documented previous research work in relation to the 3D modelling of SOFCs using COMSOL for the best of our knowledge.

1.7 Thesis Outline

This report is organized into six chapters. The first chapter provides a brief introduction to fuel cells in general and their operation along with an introduction to SOFCs. Furthermore, we have briefly described the operation of SOFCs, with the help of governing equations. Then, we have put forward our contribution and scope of work, research objectives along with the related research work regarding the SOFC fabrication and modelling.

The second chapter consists of the theoretical background information related to the thesis. We have introduced the different techniques which we have used when fabricating the SOFCs namely tape casting, screen printing and sintering along with a brief description of the measurement technique which is used during experiments.

In Chapter 3, we have given a detailed description of the SOFC fabrication process along with the assembling of SOFCs which is necessary for carrying out experiments. In addition, we have also described the experimental setup followed by the experimental procedure. Finally, we have presented how the equivalent theoretical models of the fabricated SOFCs were modelled using COMSOL.

The Chapter 4 is dedicated to document the theoretical and experimental results corresponding to the fabricated SOFCs and their equivalent COMSOL models. In this chapter, we have put forward the experimental and theoretical characteristics (polarization characteristics and power characteristics) of the fabricated and modelled SOFCs respectively.

The experimental results obtained from the fabricated SOFCs are validated in Chapter 5, by comparing them with the theoretical results. In addition, the main limitations associated with our thesis work are also discussed.

In Chapter 6, we have summarized the main findings of our thesis and pointed out our contribution to the scientific community. Finally, important extensions to the thesis are also presented in the form of future work.

In Appendix A, we have explained the equations related to the different processes associated with the COMSOL simulation model.

Finally, in Appendix B, the step by step procedure associated with modelling the equivalent SOFC models is described with the help of screenshots captured from the COMSOL Multiphysics software.

Chapter 2

Theoretical Background

In this chapter, the main focus is to provide the relevant theoretical background information regarding the thesis as a foundation to understand the SOFC fabrication and modelling which we are going to provide in the following chapters. In the first part of the chapter, we provide the fabrication processes related to SOFC electrode construction. Then, we have described the four wire measurement technique which we have used during experiments.

2.1 SOFC Electrode Fabrication

When fabricating a SOFC, we need to fabricate three electrodes namely anode, electrolyte and the cathode. We used the tape casting process for constructing the anode while the screen printing method is used to construct the electrolyte and the cathode. In order to convert the fabricated tapes (anode and electrolyte) into solid ceramics, sintering process is carried out. The following subsections describe the tape casting, screen printing and sintering processes.

2.1.1 Tape Casting Process

Tape casting (also referred to as the doctor-blade process) is the casting process used to produce thin tapes using a liquid slurry [24]. The liquid slurry contains a powder (eg: NiO_2 for anode tape), a binder, plasticisers and a solvent and mixed them together until they form a smooth mixture. A knife called *Doctors blade* and a glass plate are the main equipments used for the tape casting process. With the help of the doctors blade, it is possible to apply a thin layer of the slurry on top of the glass plate according to the required thickness of the tape. The thickness can be adjusted with the help of the adjustable blade in the doctors blade. Tape casting process is graphically illustrated in Figure 2.1.

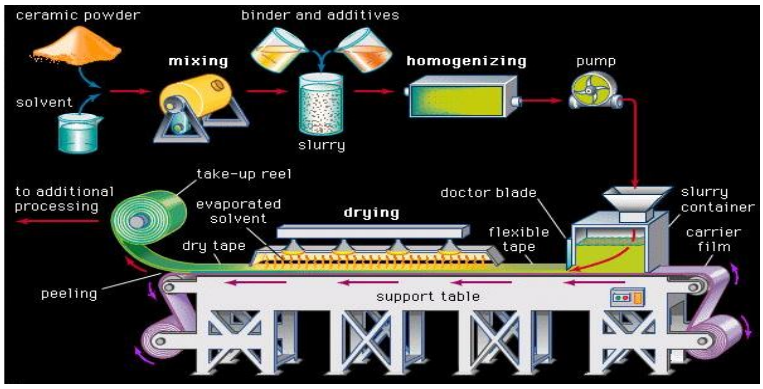

Figure 2.1: Tape casting process [3]

One of the major advantages using tape casting is that it is a low cost process for manufacturing thin ceramic films [24] [25].

2.1.2 Screen Printing

Screen printing is a method used for fabricating thick films of electrodes on top of another electrode surface. There are several advantages of screen printing method such as cheap, no need of complex machinery as well as the possibility of printing even without flat surfaces.

In order to perform the screen printing process, we need a screen, a sweeper (or a squeegee), a mesh and a printing medium. Normally, a thick liquid slurry which contains chemicals (eg: YSZ for electrolyte construction) and solvent is used as the printing medium. A popular solvent for making screen printing inks is terpineol. This is a quite viscous liquid with low vapour pressure and good wetting characteristics, but has the disadvantage of a very strong smell and is considered a hazard in chemical processing. In order to define the pattern either a square or a circle, a screen is used. Furthermore, the liquid slurry is placed on top of the screen and the sweeper is used to press the liquid slurry onto the surface making sure that an even layer is applied on top of the surface. Figure 2.2 shows the basic screen printing process. In the thesis, this method is used to fabricate the electrolyte and the cathode of our SOFCs.

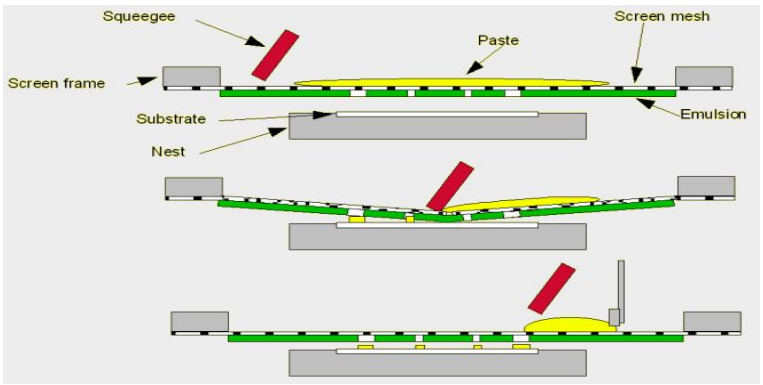

Figure 2.2: Screen printing process [4]

2.1.3 Sintering

Sintering also known as firing, is the process of compacting the ceramic powder or ceramic slurry and transform it into a solid state at a relatively high temperature. The process temperature should be below the melting point of the materials allowing to create strong bonds between particles. As a result of these bonds, the material density is increased which makes sintered ceramics suitable to be used in higher temperature applications. This is also referred to as solid state sintering [26].

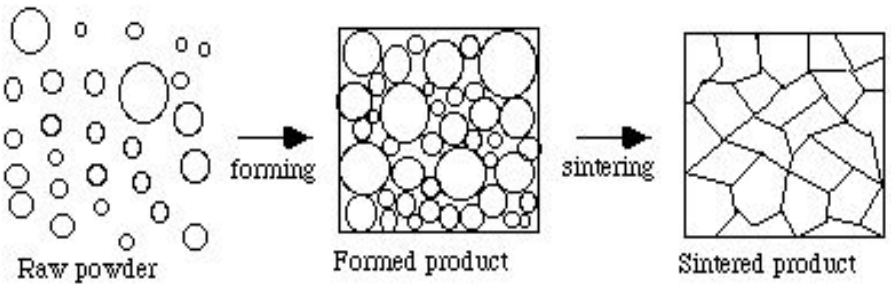

Figure 2.3: Sintered process [5]

2.2 Measurement Techniques

In the following subsection, we describe the measurement technique which we applied when obtaining the current-voltage characteristics of the experimental SOFCs.

2.2.1 Four Wire Measurement Technique

The 4-wire method for measuring accurate voltage is much preferred over 2-wire measurements that are obtained with a normal multimeter. The essence of the 4-wire method is to have separate current and voltage wires that connect together at a point as close as possible to the desired measuring point. In the case of an SOFC single cell, the electrodes are made with separate voltage and current wires which are then fed though the apparatus to the instrumentation to achieve the desired 4-wire measurement. This then eliminates almost all of the ohmic drop that would otherwise be seen in the current wires.

The 2-wire method is shown in Figure 2.4.

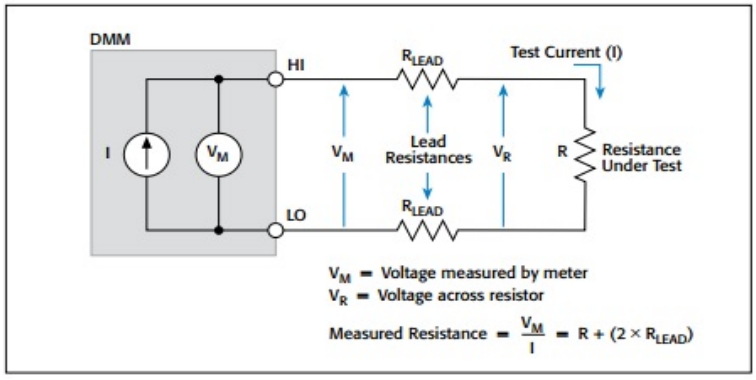

Figure 2.4: 2-wire measurement technique [6]

Here, the voltmeter reading (V_M) is not exactly same as the voltage across the SOFC (V_R). The voltage drop of the wires needs to take into account resulting the V_M is greater than the V_R.

The complementary 4-wire method is shown in Figure 2.5. In order to avoid the ohmic loss issue, the voltmeter and an ammeter are used to measure the voltage and current separately.

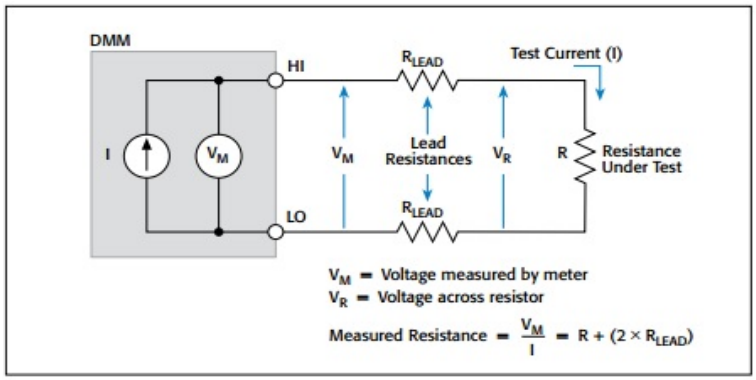

Figure 2.5: 4-wire measurement technique [6]

In this method, there are two sets of wires used for the voltmeter and the ammeter connections. The current through the ammeter is high while the current through the voltmeter is very low. Therefore, V_M is approximately equal to V_R [27].

Chapter 3

SOFC Fabrication and Modelling

This chapter provides the fabrication procedure of our fabricated SOFCs in a descriptive manner. In addition, we have described the procedure associated with assembling of the SOFC for the experiments followed by the experimental setup and the experimental procedure. Finally, we mention the modelling process of theoretical models equivalent to the fabricated SOFCs to obtain the theoretical characteristics.

3.1 Fabrication Methodology with Tape Casting and Screen Printing

ASCs require a thick and mechanically strong support onto which the other much thinner layers are screen printed. Tape casting has been selected as the method for making the anode support.

First we fabricated the anode using the tape casting process. Then, the cathode, active layer, electrolyte, barrier layer and the cathode are screen printed as separate stages. The overview of fabrication procedure is shown in Figure 3.1.

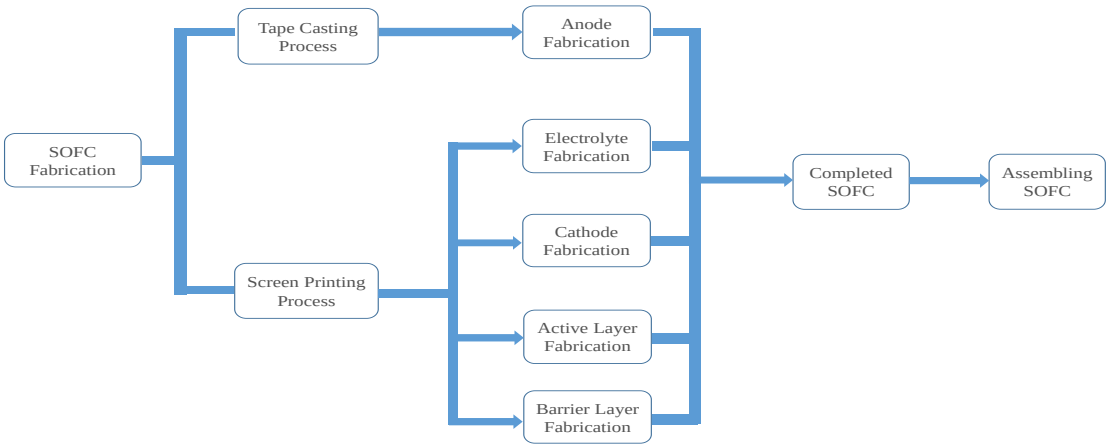

Figure 3.1: The overview of fabrication procedure

In order to make a working cell we have considered five layers as given in Figure 3.2. First, we fabricate the porous anode using tape casting. We have used NiO_2 with large particle sizes (see table for D_{50} values) to make sure that the sintered substrate is porous enough to allow H_2 gas to pass through. In the "green" state the tape is casted at about 1 mm in thickness, but will later shrink down to around 0.3 mm after sintering. In this study, we use a co-firing strategy in which the substrate and intermediate active layers are co-sintered. The final cathode layer is then screen printed and sintered in a separate firing cycle.

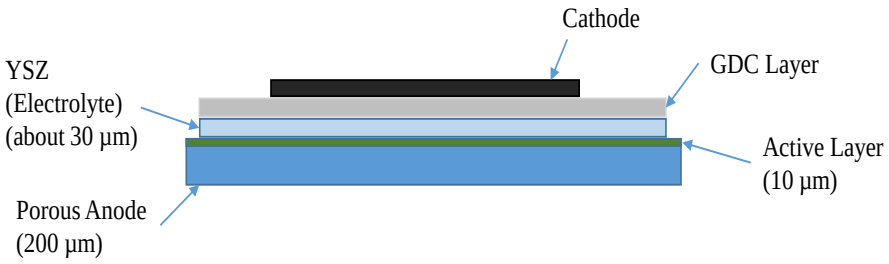

Figure 3.2: The cross section of a fabricated SOFC single cell

The next layer is an active layer which contains smaller particles of NiO_2. The reason for using finer particles of NiO_2 (as mentioned in Table 3.1) is to increase the number of triple phase boundary points. On the other hand the larger particles of NiO_2 are to ensure adequate porosity in the substrate to ensure free diffusion H_2. This layer is screen printed on top of the porous anode ensuring that it has a thickness about 10 μm. The electrolyte (which contains YSZ) is screen printed on top of the active layer. Before we screen print the cathode, a thin layer of Gadonium doped Ceria (GDC) (consisting of Gadolinium(III) Oxide (Gd_2O_3) and Cerium Dioxide (CeO_2)) is first screen printed on top of the electrolyte. This layer acts as a barrier to prevent the reaction of Lanthanum Strontium Cobalt Ferrite (LSCF) ($LaSrFeCoO_3$ - the cathode ink) with the YSZ (Zirconium Dioxide (ZrO_2) and Y_2O_3) of the electrolyte. Note that, if we allow this reaction to occur, it will create an insulation layer of Strontium Zirconate ($SrZrO_3$) between the electrolyte and the cathode.

3.2 Water based Formula for Tape Casting

Our main objective was to develop a water based tape casting slurry that avoids using organic solvents. This meant that we have to select binders and plasticisers and dispersants that are water compatible and allow a uniform a stable film to be formed after the slurry has been tape casted.

To make a stable tape cast slurry we need to have 4 components Binder, Plasticiser, Dispersant and Solvent (water in this case). We then add the ceramic powder to the recipe to complete the formula. Typically, the ceramic content is around 80% by weight.

1. *Binder:* PVA-polyvinyl alcohol is a common binder that is soluble in water up to 40% and when dry it can form a stable adherent film when cast onto glass. This was selected as our main choice. In our case, we made a stock solution of 20 % which was then added in various proportions to make a particular batch for casting. Adding too much binder will cause excessive shrinkage during the sintering process.

2. *Plasticiser:* Glycerol is a very good choice as it is non-toxic, safe and dissolves in water in all proportions. It has a relative low vapour pressure and this makes a tape that can remain stable in air for several weeks before becoming too brittle.

3. *Dispersant:* The dispersant is necessary to ensure that the ceramic particles do not form agglomerates. A low foaming surfactant such as Tween 80 is a suitable choice as it is miscible in water. Only a small addition is required around 1% of the weight of ceramic powder. The dispersant is added to the ceramic powder during the ball milling stage. This ensures that the slurry will be free from agglomerates.

3.3 Cell Fabrication Procedure

We have fabricated two SOFCs which we denote as $SOFC_A$ and $SOFC_B$. The difference between these two SOFCs are the chemical composition used for the construction of the anode and the electrolyte. The percentage of chemicals we used for fabrication of both $SOFC_A$ and $SOFC_B$ are shown in Table 3.1. The detailed description for fabrication of two SOFCs are mentioned below. The term "polymer" in the table refers to the combined binder, plasticiser and dispersant combination.

Table 3.1: Comparison of chemical compositions of SOFCs (wt%)

		$SOFC_A$	$SOFC_B$	Particle Surface Area (m^2/g)	Particle Density (μm)
Porous Anode	NiO_2	60%	55%	7.23	0.63
	$3YSZ$ $(3Y)$	40%	50%	11	0.43
	Polymer	30%	40%	-	-
Active Layer	NiO_2	60%	55%	8-12	0.3-0.6
	$3YSZ$ $(3Y)$	40%	50%	11	0.43
	Polymer	30%	40%	-	-
Electrolyte	$8Y$	75%	75%	8.3	0.45
	Polymer	25%	25%	-	-
GDC Layer	20 GDC	46%	46%	-	-
Cathode	$LSCF$	53%	53%	-	-

3.4 Fabrication of $SOFC_A$

In the following subsections, we discuss the procedure which we followed when fabricating the $SOFC_A$.

3.4.1 Anode Fabrication

As stated in Table 3.1, we need three chemicals. In addition to that we need water as a solvent. The procedure associated with fabricating the anode tape is as follows.

First of all, we put all the chemicals (NiO_2, $3Y$ and polymer) into a container and add 5 g of water and mixed them until dissolved. We used an electric mixer to mix the chemicals together for 1 *hour* forming a viscous liquid called the *slurry*. Finally, with the help of a vacuum chamber, we removed the air bubbles in the slurry we made for the anode. The procedure mentioned is also described with the help of the Figures 3.3, 3.4 and 3.5.

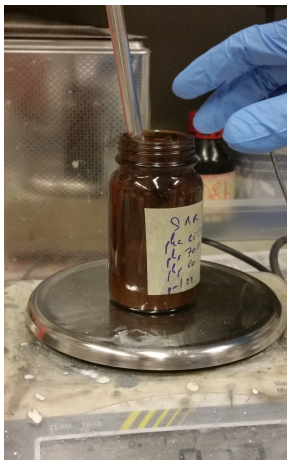

Figure 3.3: Measuring the chemicals

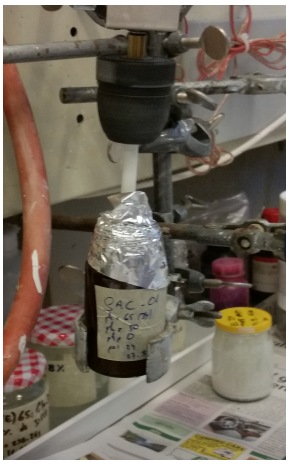

Figure 3.4: Mixing the chemicals using an electric mixer

Figure 3.5: Removing the air bubbles

Next step is the construction of a tape for the anode. For this process, we need the slurry made earlier, a glass plate and a doctors blade. The prepared slurry is placed on top of the glass plate. By using the doctors blade, the slurry was spread along the glass plate by gliding it on top of the plate in such a way that the tape is having 1 mm of thickness. This process is called as the tape casting process which is shown in the Figure 3.6.

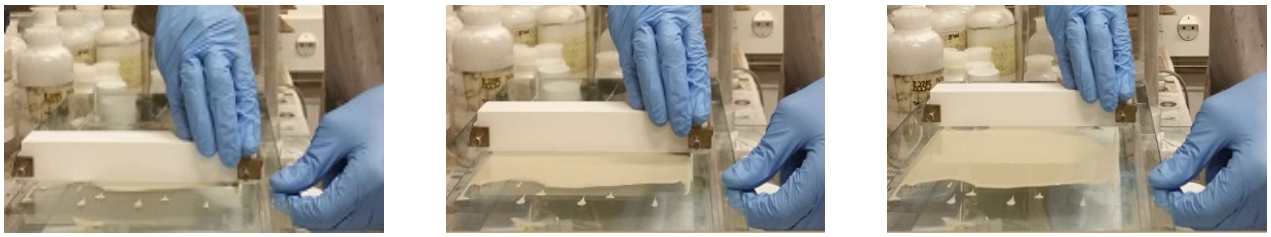

Figure 3.6: Tape Casting Process

Then, we let the prepared tape to be dried out in air for few hours. The fabricated anode tape is shown in Figure 3.7. Then, the tape was removed carefully with the help of a scraper.

Figure 3.7: Fabricated anode tape using tape casting process

3.4.2 Electrolyte Fabrication by Screen Printing

In order to fabricate the electrolyte (on top of the anode tape), first we make a thick slurry using the pure $8Y$ (8% of Yttrium of Y_2O_3), polymer and water as solvent and the percentages of the chemicals used are mentioned in Table 3.1. The process of making the slurry for the electrolyte is similar to the process of making the slurry for the anode as given in Section 3.4.1.

Before we fabricate the electrolyte on top of the anode, first a thin layer of NiO_2 is screen printed (using the previously made anode slurry) on top of the anode tape. This layer helps in improving the current collection capability of the SOFC. For the screen printing process, a printing medium (in this case the anode slurry), a screen, a mesh and a sweeper are required. The sweeper and the mesh which is required to apply an even layer of the slurry on top of the anode are shown in the following Figures 3.8 and 3.9.

Figure 3.8: The sweeper used to spread the paste

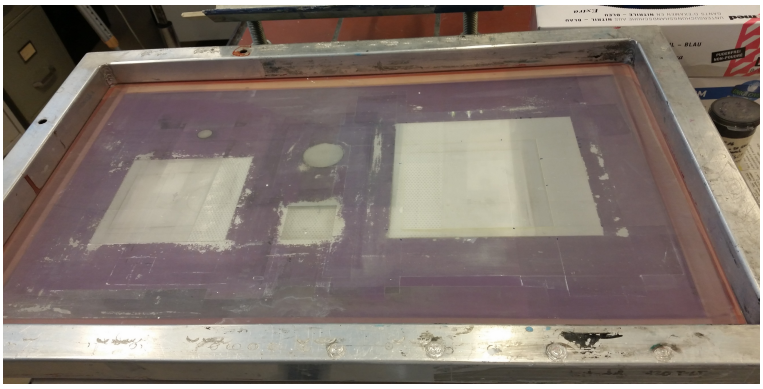

Figure 3.9: The mesh with the required pattern

Furthermore, it is necessary to keep a constant distance between the mesh and the cell to have a consistent layer. The setup which is used for the screen printing, including the mesh is illustrated in Figure 3.10. After screen printing the layer of NiO_2 on top of the anode tape, the electrolyte is screen printed on top using the electrolyte slurry (made of pure $8Y$) as the printing medium. The detailed description of the screen printing method is given in Section 3.4.3 when we describe the screen printing of the cathode.

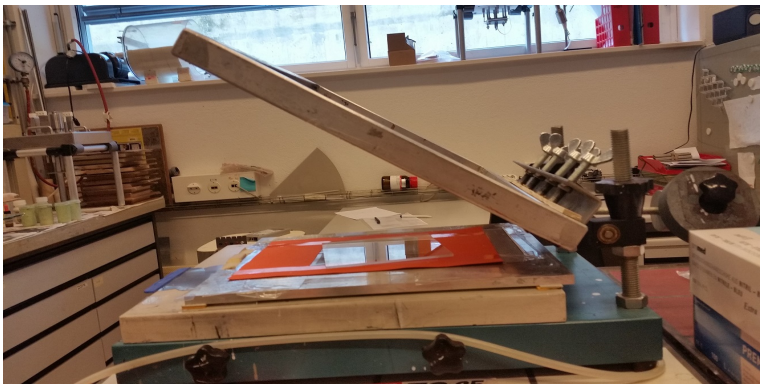

Figure 3.10: Setup for the screen printing

Next step is to convert the fabricated tape into a ceramic. In order to do this, we used the sintering process described in Section 2.1.3 and thereby increase the temperature of the SOFC in a systematic way (with the help of a temperature curve) as shown in Figure 3.11. First, we increased the temperature up to $750°C$ (with the rate of $15°C/hour$) and left the fabricated tape at $750°C$ for 2 $hours$ to allow the polymer to be burnt out completely. Then, we increased the temperature up to $1300°C$ and left 15 $hours$ to solidify the tape. Finally, the temperature is reduced to room temperature at a rate of $100°C/hour$.

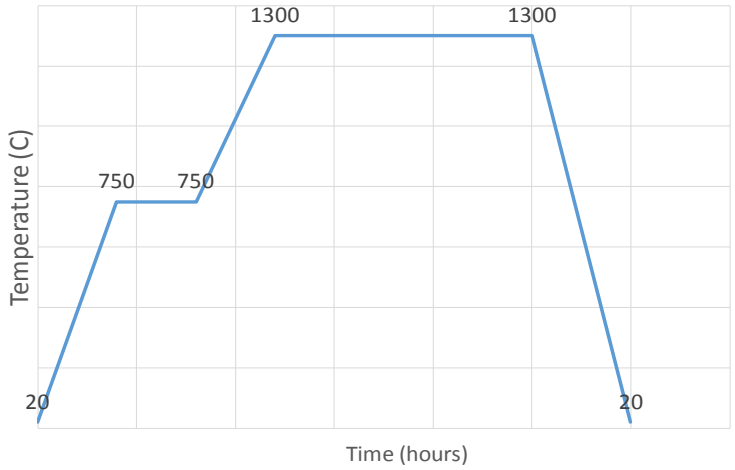

Figure 3.11: Temperature curve for sintering process

The final ceramic tape (both the anode and the electrolyte) after the sintering process is illustrated in Figure 3.12.

Figure 3.12: Fabricated tape after sintering process

3.4.3 Cathode Fabrication and Application

The cathode was made as a separate slurry using a method similar to the tape casting procedure. In our case, we selected $LSCF$ as the cathode material as it has been shown to be very active in the temperature range that we are using in our tests ($750°C$ - $800°C$).

The associated steps in screen printing of the cathode (on top of the layer of GDC) is illustrated with the help of the Figure 3.1.A to Figure 3.1.G respectively.

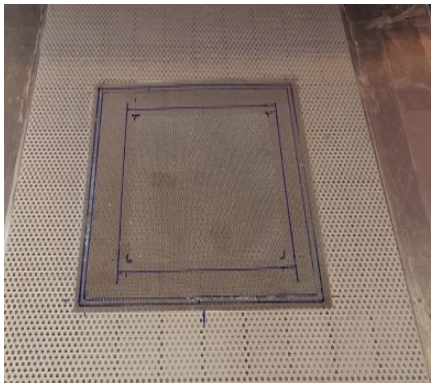

Figure 3.1.A shows the base plate of the screen printer.

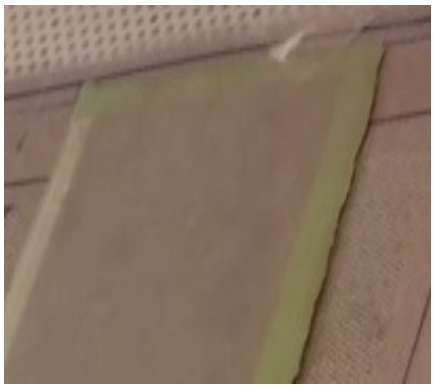

Figure 3.1.B illustrates the placing of the sintered cell on top of the base plate with the electrolyte side on top.

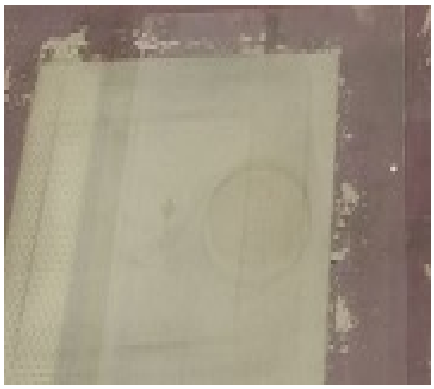

Figure 3.1.C shows the required mask pattern for the cathode either round shape or square shape. In this case, we used round shape with a diameter of 50 mm. In order to achieve this, the required shape is carved on top of the tape and stick it on top of the mesh.

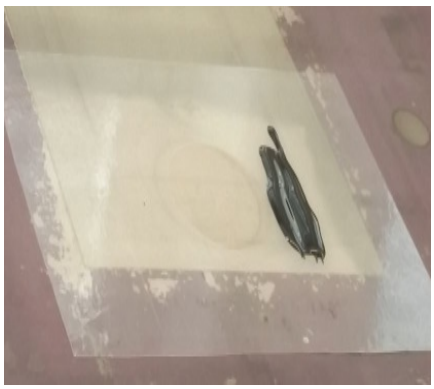

Figure 3.1.D illustrates the place where to apply the cathode ink on top of the mesh to perform screen printing. As the cathode ink, we have used LSCF.

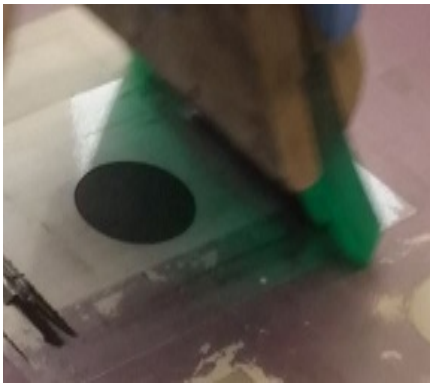

Figure 3.1.E illustrates the procedure of screen printing. The ink needs to press towards the cell which is on top of the base plate. The sweeper (squeegee) is used to press the ink.

Figure 3.1.F shows the final position of the sweeper after finishing screen printing. It is obvious to make sure that an even layer of ink is applied.

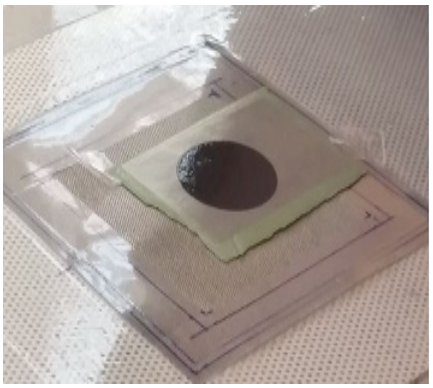

Figure 3.1.G illustrates the fuel cell after the screen printed cathode has been applied.

3.5 Fabrication of $SOFC_B$

The fabrication procedure for the anode, the electrolyte and the cathode for $SOFC_B$ are identical to the fabrication process of $SOFC_A$. Note that, the only difference between the two SOFCs is the chemical compositions used for the construction of the anodes in respective SOFCs.

3.6 Assembling the SOFC

After making the cells, the next stage is to test them in the SOFC setup. This comprises of a furnace able to achieve $1300°C$, a gas mixing station and instrumentation to measure the cell characteristics.

The associated procedure is described with the help of the following Figures.

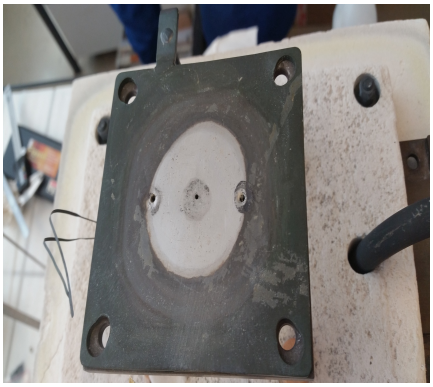

Figure 3.2.A shows the base plate of the experimental setup with H_2 intake for the anode.

Figure 3.2.B shows the compressed Nickel foam placed on top of the setup which has a thickness about $0.5\,mm$. This Nickel foam helps to distribute H_2 throughout the surface of the anode.

Figure 3.2.C illustrates the sealing gel which is used in between the plate and the insulation layer to make sure that there is no leakage.

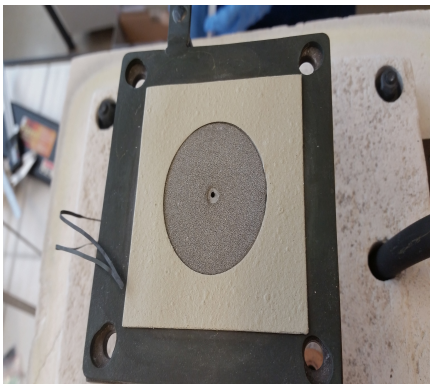

Figure 3.2.D shows the placed single insulation layer on top of the sealing gel assuring that there is no gap between the plate and the insulation layer. Moreover, this layer prevents contacting any corner of the anode with any metal parts of the setup.

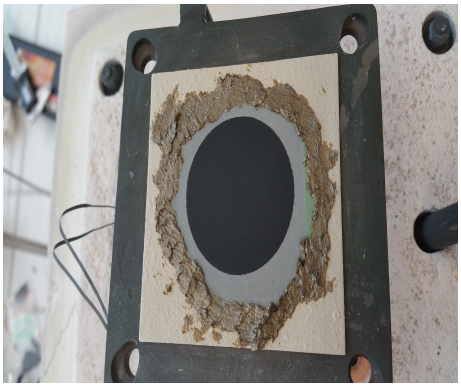

Figure 3.2.E illustrates the SOFC on top of the insulation layer. The sealing gel is applied around the SOFC to ensure that there is no leakage.

Figure 3.2.F shows the gold current collector which is placed on top of the cathode and the upper insulation layer around the SOFC.

Figure 3.2.G illustrates the thermocouple connectors which are connected to the cell in order to measure the actual cell temperature. Furthermore, the insulation cap is placed on top of the cathode.

Figure 3.2.H shows the final insulation layer placed on top to cover all the components.

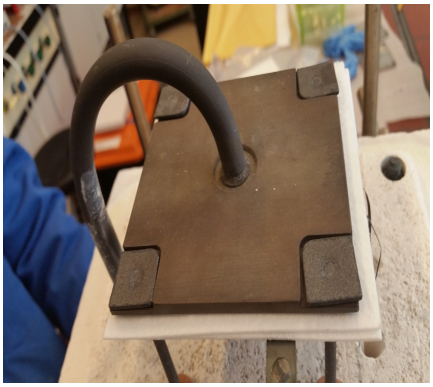

Figure 3.2.I shows the final plate of the setup which contains air intake for the cathode.

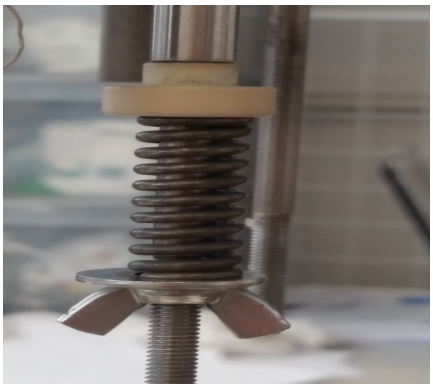

Figure 3.2.J illustrates a close-up picture of the screw going through the assembly. The pressure applied to the SOFC during the experiment depends on the length of the spring. Therefore, it is necessary to have the same distance for all the four springs in the setup. The set of 4 springs is used to apply the correct amount of pressure that is require to make good ohmic contact between the mesh current collectors and the cell under test. In our setup, each spring is 26.45 mm in length.

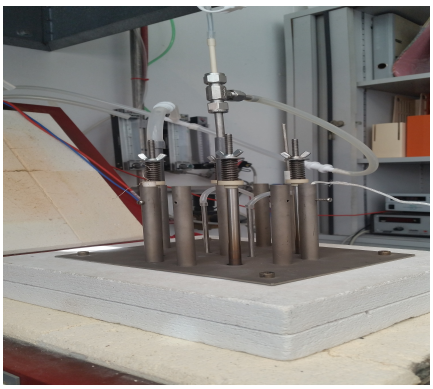

Figure 3.2.K shows the final experimental setup which is placed in the furnace to increase the temperature to the operating temperature of the SOFC prior to perform the experiments.

3.7 Experimental Setup

In order to carry out the experiments on the fabricated SOFCs, first an experimental setup is formed as mentioned below. The setup includes a furnace, two digital multimeters, a power supply, a thermocouple, a gas flow controller and a temperature controller. Given that a single SOFC produces low power, we have connected the power supply in series with the SOFC.

Furthermore, we have used the 4-wire measurement technique (as described in Section 2.2.1) to measure the voltage of the SOFC. Figure 3.13 illustrates the equipment layout whereas Figure 3.14 shows the snapshot of our experimental setup.

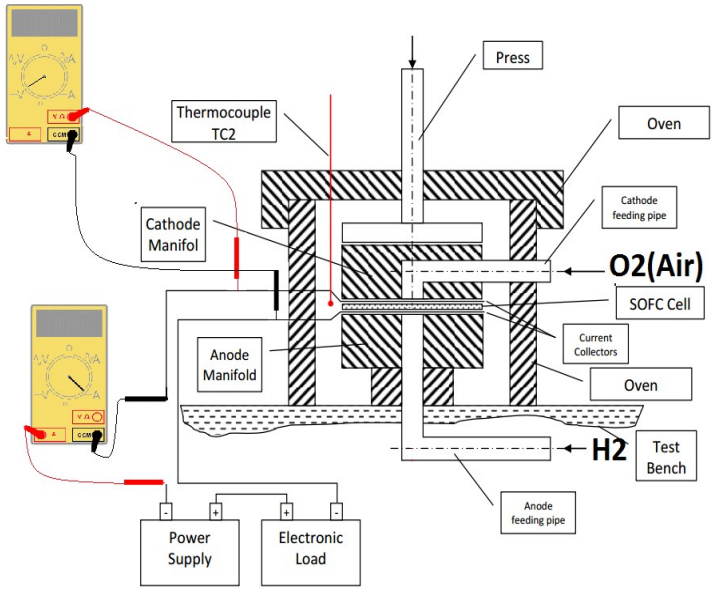

Figure 3.13: Equipment layout for the experimental setup [7]

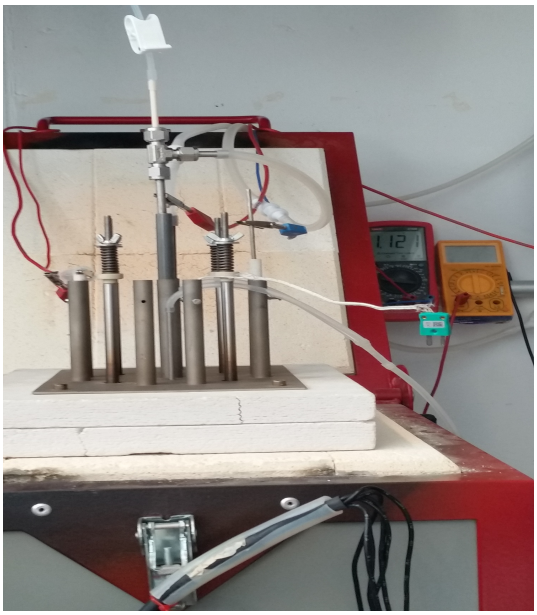

Figure 3.14: Snapshot of our experimental setup

3.8 Components used for Experimental Setup

This section describes the functionality of the components used in the experimental setup.

3.8.1 Temperature Controller

It is necessary to keep the SOFC within the operating temperature which is $755°C$. Hence, we increased the temperature from room temperature to the operating temperature of the SOFC using the temperature controller. We did not increase the temperature instantly to $755°C$. The temperature was increased according to a temperature curve shown in Figure 3.15. Then, we kept the temperature at $755°C$ during the experiments, which is the operating temperature of the SOFC.

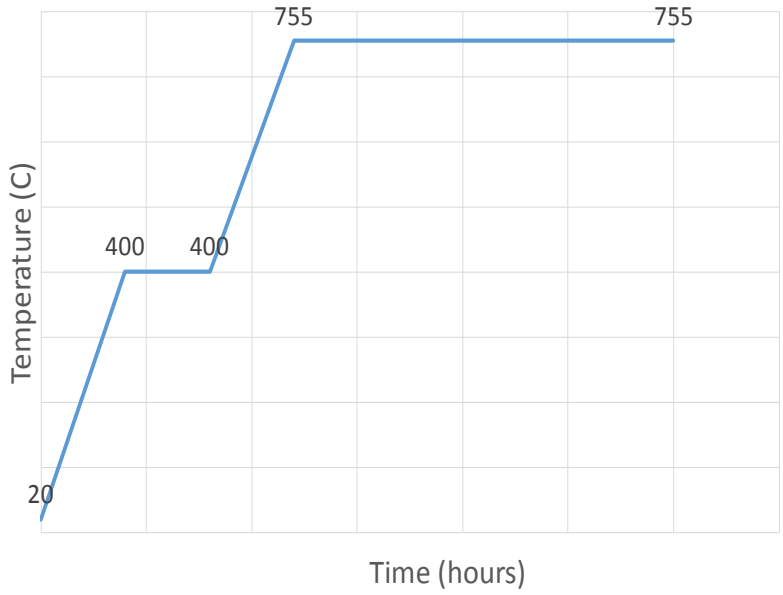

Figure 3.15: The temperature curve for raising the temperature of the SOFC to $755°C$

3.8.2 Gas Flow Controller

Gas flow controller is used to control the flow of gases. For the experiments, we have used three channels of the controller to pump the gas as the fuel to the SOFC. Those channels are used to control the flow of H_2, Nitrogen (N_2) and air. The reason for inserting N_2 is to prevent the reaction of H_2 and O_2 from air. If we inserted H_2 and air directly to the system, they will react and ultimately damage the SOFC.

3.8.3 Thermocouple

Although, we program the temperature controller to a certain temperature ($755°C$) as the operating temperature, this might not be the actual temperature of the SOFC inside the furnace. With the help of a thermocouple attached to the SOFC, we can measure the actual temperature of the SOFC. Thus, it is possible to adjust the temperature through the temperature controller until the thermocouple shows the value $755°C$.

3.9 Experimental Procedure

In this section, we have described the experimental procedure we used for our experiments. We have inserted air to both the anode and the cathode electrodes of the SOFC until temperature reaches from room temperature to $755°C$. Then, we fed N_2 to the anode side while air supply remains the same in the cathode side. Finally, we have replaced N_2 with pure H_2 and let the system run for 30 $minutes$ to have a steady open circuit voltage (OCV). In order to obtain the cell characteristics, we have decreased the voltage of the SOFC by steps of 50 mV from OCV to 450 mV and obtained the corresponding current values. In order to evaluate the performance of the fabricated SOFCs, the following characteristics are considered.

- Polarization curve (SOFC Voltage vs Current density)
- Power curve (Power density vs Current density)

The obtained cell characteristics and cell data are presented in Chapter 4.

3.10 Theoretical Model

In order to validate the performance of the fabricated SOFCs, we developed theoretical models equivalent to the fabricated SOFCs using the COMSOL software. The following subsection describes the construction of the equivalent COMSOL models.

3.10.1 Model Construction

The first step is to construct the geographical model. We have selected *y-z plane* as the 2D plane for our model. Then by using rectangle shapes, we constructed the cross section of the 2D model as shown in Figure 3.16.

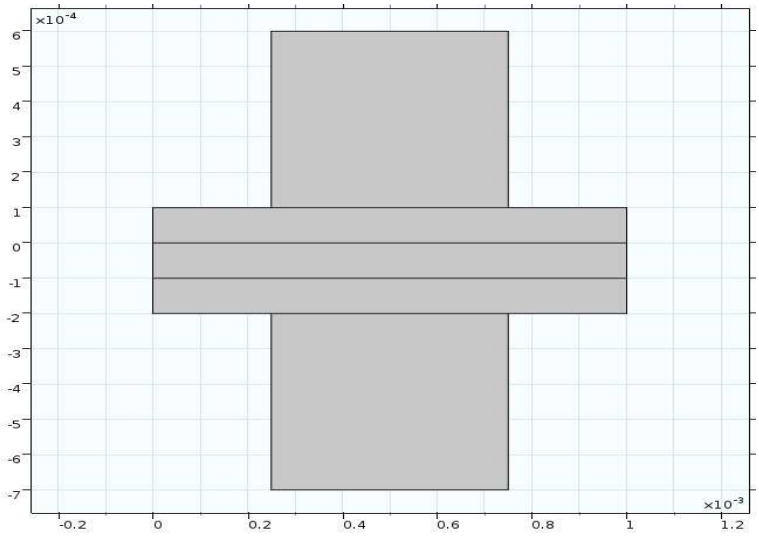

Figure 3.16: Constructed 2D model

For this model, we used two porous gas diffusion electrodes (GDEs) as the anode and the cathode. Furthermore, the anode flow channel, cathode flow channel and the electrolyte were also included. Then, we extruded it to generate the 3D model. The constructed 3D geographical model is shown below.

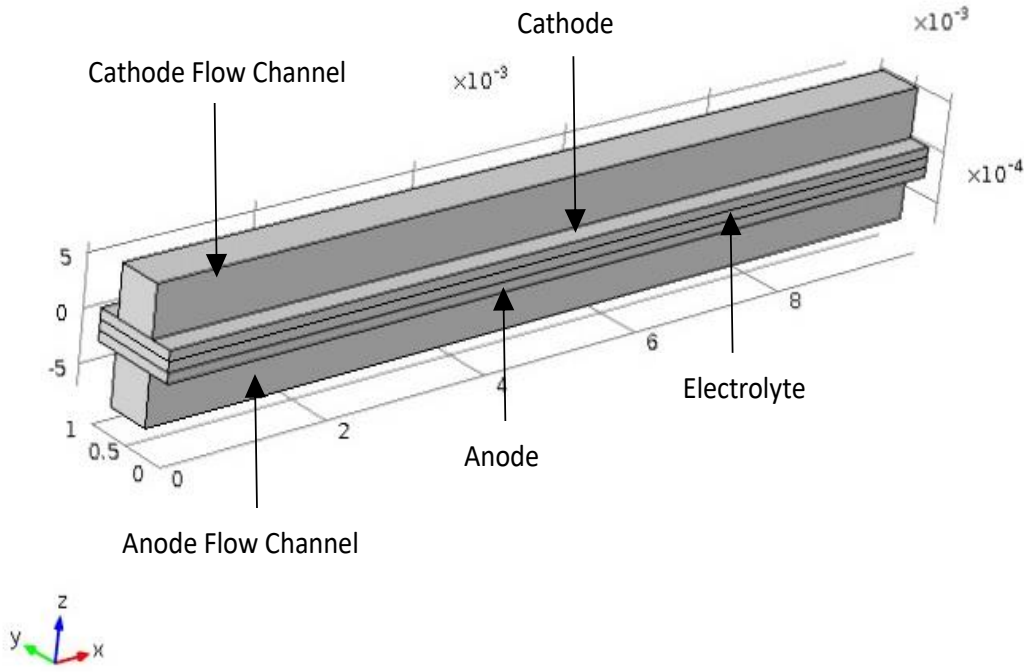

Figure 3.17: Constructed geometry for the model

The next step is to configure the model according to our requirements. In order to achieve that, we need to select the appropriate physics related to the model. We have defined mass

fractions for the anode and the cathode of the model by using the physics related to the chemical species transport. Then, the related velocities and the pressure for both the anode and the cathode are defined by using free and porous media flow. Furthermore, we have considered that the H_2 rich gas is entering to the anode from the left while air is fed from the right of the cathode. We have used the secondary current distribution for two porous GDEs and for the electrolyte. Then, we need to set the parameters for the electrodes and for the anode flow channel as well as the cathode flow channel. The relevant parameters are given in Table 3.2.

Table 3.2: Parameters used for the model

Description	Value		Description	Value
Atmospheric pressure	1.013e5 Pa		Kinetic volume H_2	$1e-6$
Temperature	$755°C$		Kinetic volume O_2	$1e-5$
Viscosity, air	$3e-5$ $Pa.s$		Kinetic volume N_2	$6e-6$
Pressure drop, anode	2 Pa		Kinetic volume H_2O	$1.7e-6$
Pressure drop, cathode	6 Pa		Molar mass, H_2	2 g/mol
Exchange current density, anode	0.1 A/m^2		Molar mass, H_2	2 g/mol
Exchange current density, cathode	0.01 A/m^2		Molar mass, O_2	32 g/mol
Specific surface area, anode	200 $1/m$		Molar mass, N_2	14 g/mol
Specific surface area, cathode	200 $1/m$		Molar mass, H_2O	18 g/mol
Initial cell polarization	0.05 V		Reference diffusivity	$3.16e-8$ m^2/s
Anode permeability	$1e-10$ m^2		Porosity	0.4
Cathode permeability	$1e-10$ m^2		Diffusivity, H_2-H_2O	0.0010759 m^2/s
Equilibrium voltage, anode	0 V		Diffusivity, O_2-H_2O	$2.0927e-4$ m^2/s
Equilibrium voltage, cathode	1 V		Diffusivity, O_2-N_2	$2.5329e-4$ m^2/s
Cell voltage	0.95 V		Diffusivity, N_2-H_2O	$2.8882e-4$ m^2/s
Electrode effective conductivity, anode	1 S/m		Gas flow channel width	$5e-4$ m
Solid effective conductivity, anode	1000 S/m		Rib width	$5e-4$ m
Electrode effective conductivity, cathode	1 S/m		Gas diffusion electrode thickness	0.001 m
Solid effective conductivity, cathode	1000 S/m		Electrolyte thickness	0.001 m
Electrolyte conductivity	25 S/m		Gas flow channel height	$5e-4$ m
Current collector conductivity	5000 S/m		Flow channel lenght	0.01 m
Inlet weight fraction, H_2-H_2O	0.4		Inlet weight fraction, O_2-H_2O	0.15
Inlet weight fraction, O_2-N_2 y	0.37		Total molar concentration	11.853 mol/m^3

After configuring the parameters, we have created the mesh to discretize the model. We used finite element method which divides the model into small geometrical shapes. Hence, we can get more accurate results for our simulations. The constructed mesh for the model is shown in Figure 3.18.

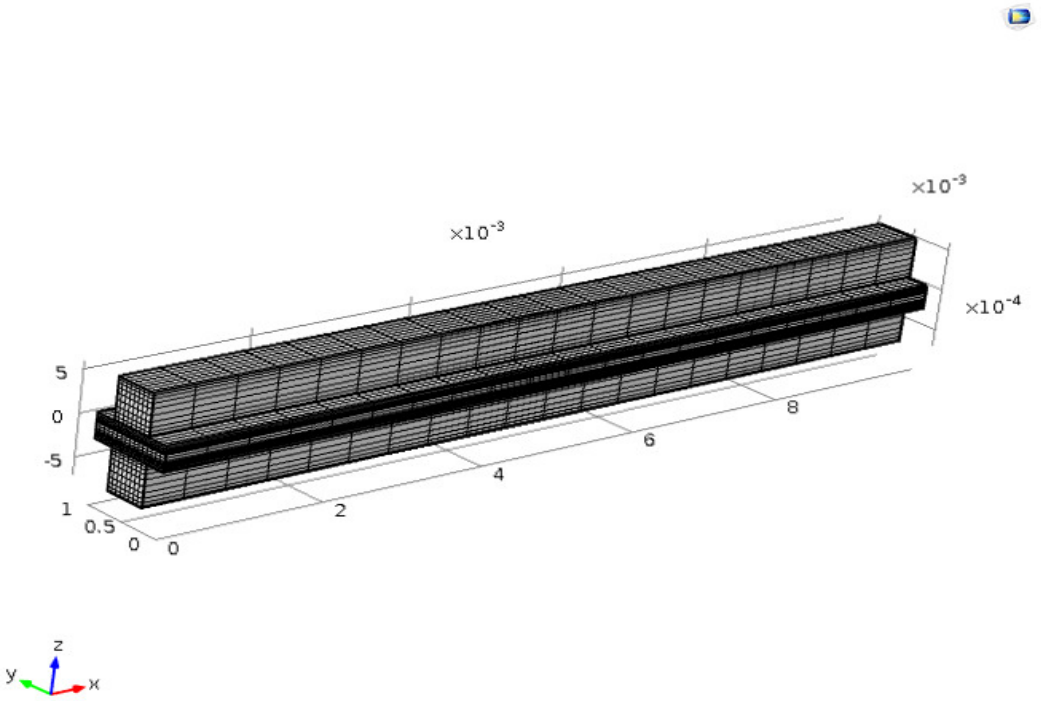

Figure 3.18: Constructed Mesh for the Model

As the final step, we need to obtain the theoretical characteristics of the modelled SOFC. In order to do that, we need to define the mode of study. For our analysis, we selected the stationary study mode assuming that the load and temperature are independent of the time. Finally, the model was simulated to obtain the theoretical SOFC characteristics.

Chapter 4

Theoretical and Experimental Results

In this chapter, our main focus is to illustrate the theoretical and experimental results of the newly constructed SOFCs and the equivalent theoretical COMSOL simulation models. First, we provide the corresponding results for the fabricated SOFCs and then the simulation results obtained from the equivalent COMSOL models are presented.

4.1 Experimental Results

In this section, we have provided the experimental results obtained in relation to $SOFC_A$ and $SOFC_B$. First, the polarization curves for both SOFCs are presented followed by the power curves.

4.1.1 Polarization Curves for $SOFC_A$ and $SOFC_B$

Figure 4.1 and Figure 4.2 shows the polarization curves plotted for $SOFC_A$ and $SOFC_B$ respectively.

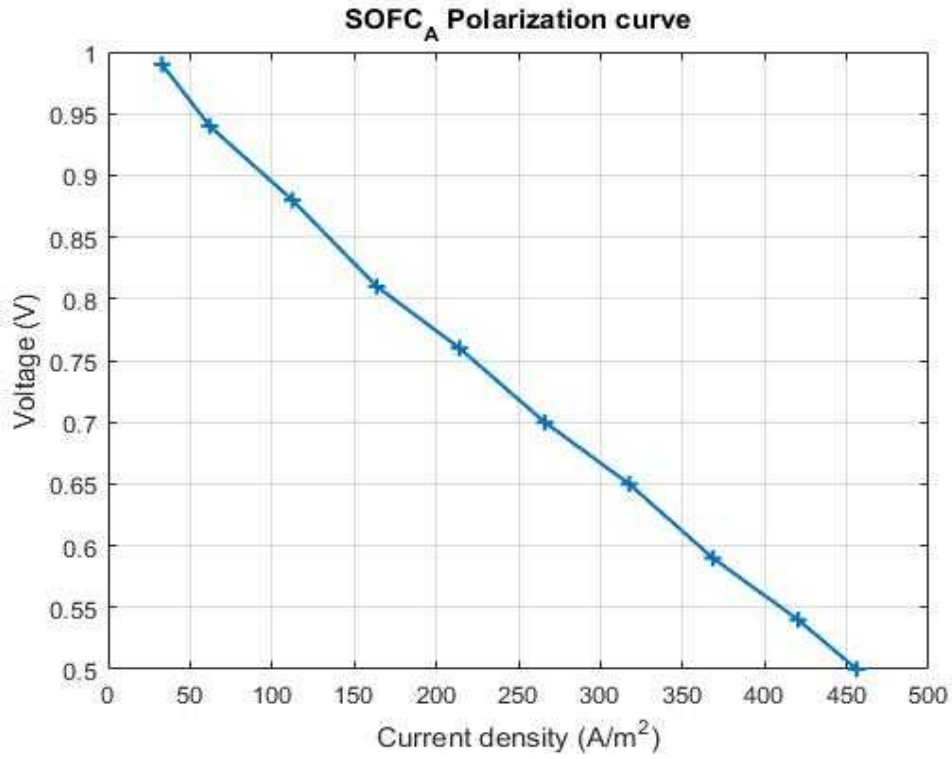

Figure 4.1: Voltage vs Current density for $SOFC_A$

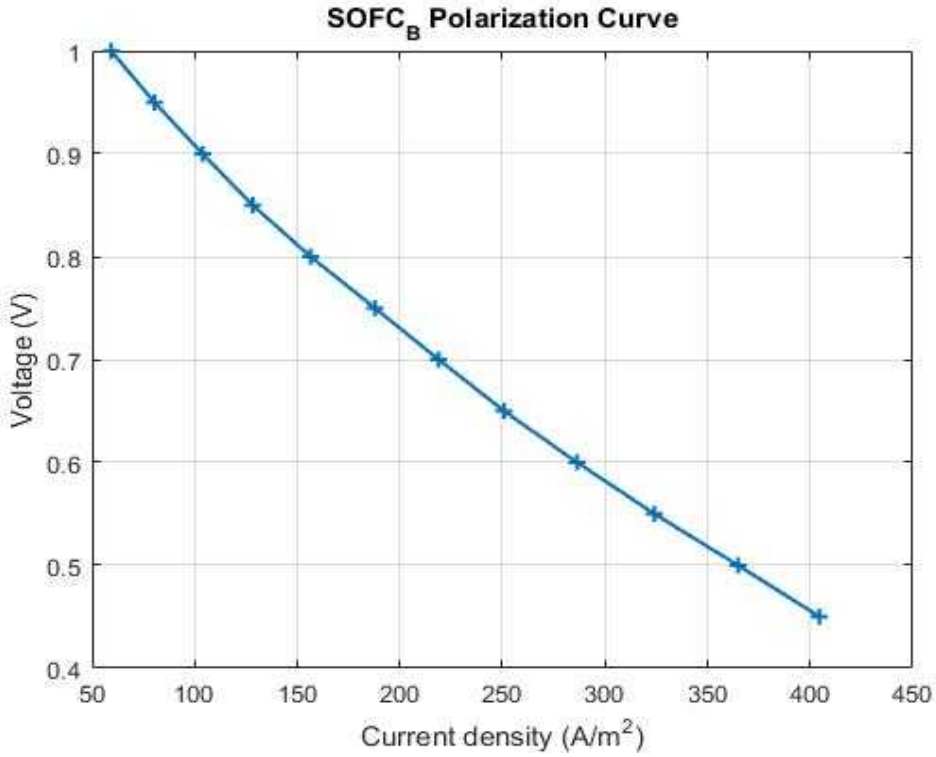

Figure 4.2: Voltage vs Current density for $SOFC_B$

4.1.2 Power Curves for $SOFC_A$ and $SOFC_B$

Figure 4.3 and Figure 4.4 shows the power curves plotted for $SOFC_A$ and $SOFC_B$ respectively.

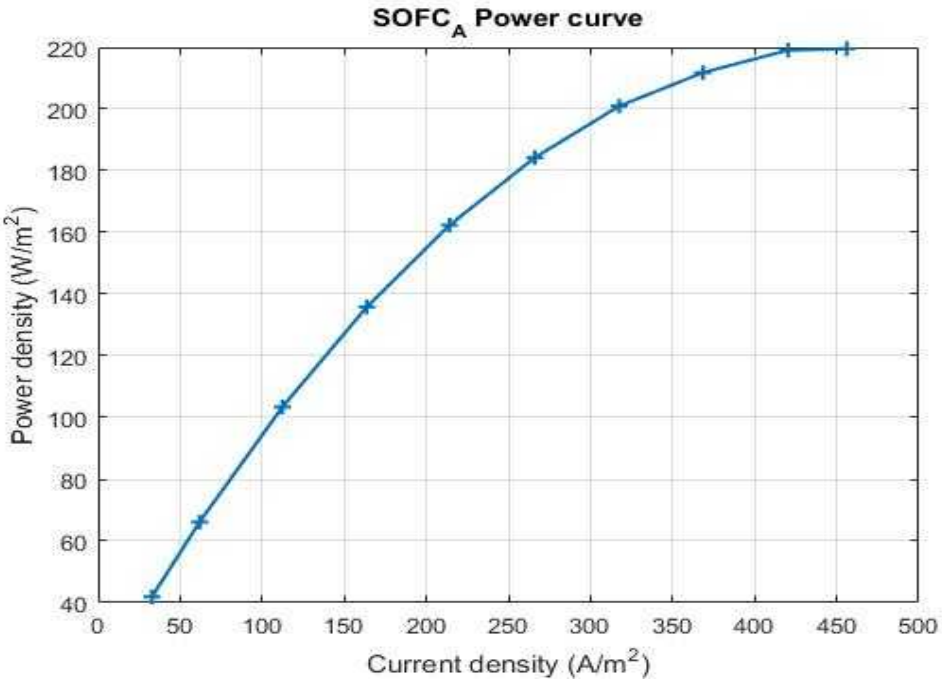

Figure 4.3: Power density vs Current density for $SOFC_A$

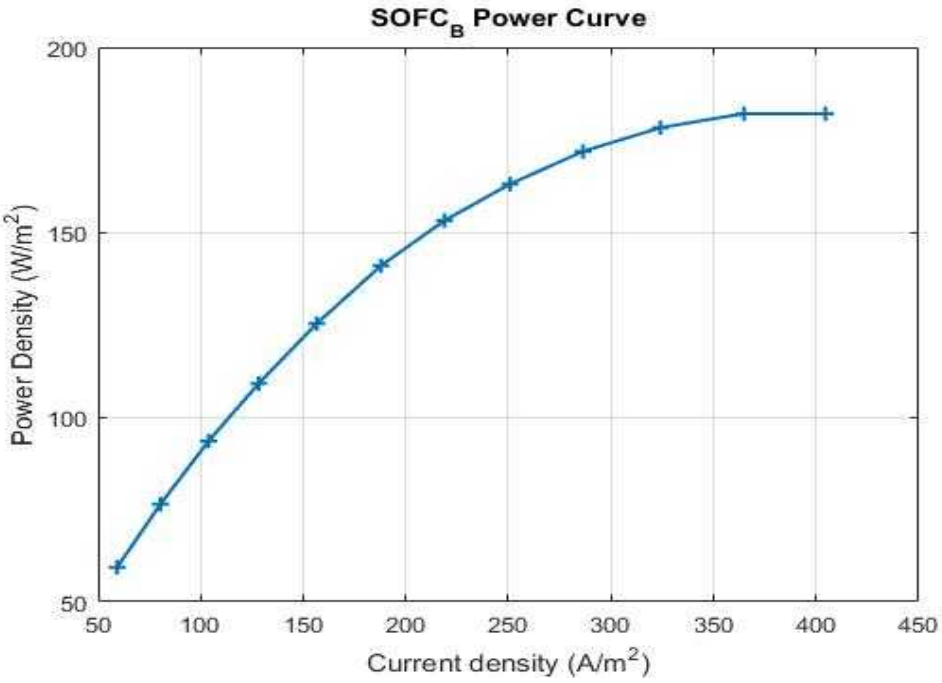

Figure 4.4: Power density vs Current density for $SOFC_B$

4.2 Theoretical Results

This section provides the simulation results we have obtained through simulating the COMSOL models which are equivalent to $SOFC_A$ and $SOFC_B$. We have developed two COMSOL models equivalent to both $SOFC_A$ and $SOFC_B$ by changing the parameters of the model.

4.2.1 Current Density Distribution

The following figures show the current density distribution of the cathode side along the *z direction*.

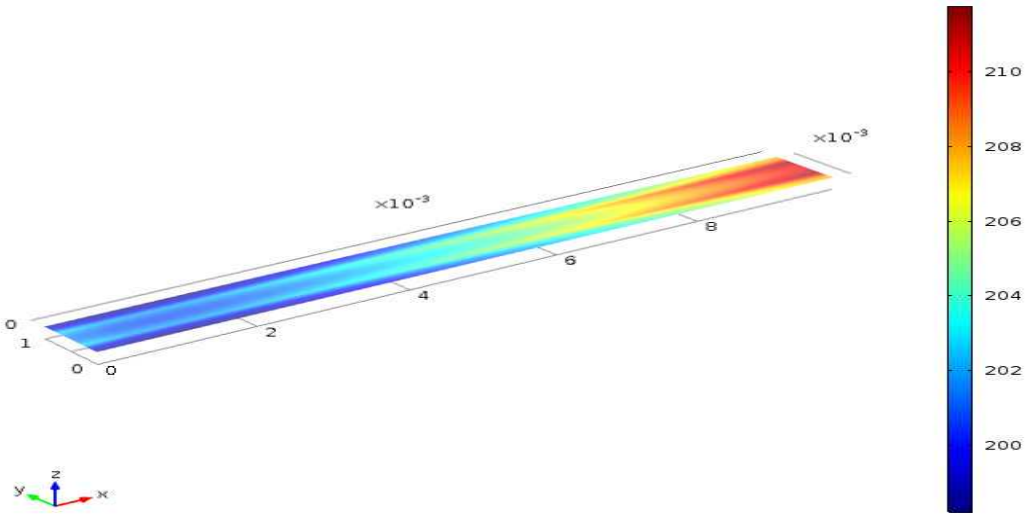

Figure 4.5: The Current density of $SOFC_A$

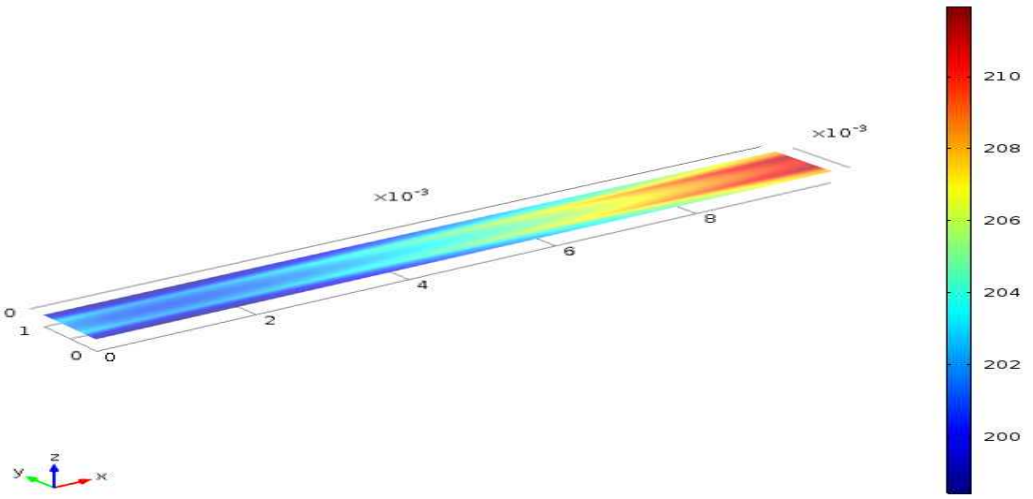

Figure 4.6: The Current density of $SOFC_B$

4.2.2 Polarization Curves for the Theoretical Models

The variation of voltage with current density obtained from the simulation of equivalent COMSOL models for $SOFC_A$ and $SOFC_B$ are shown in Figure 4.7 and Figure 4.8 respectively.

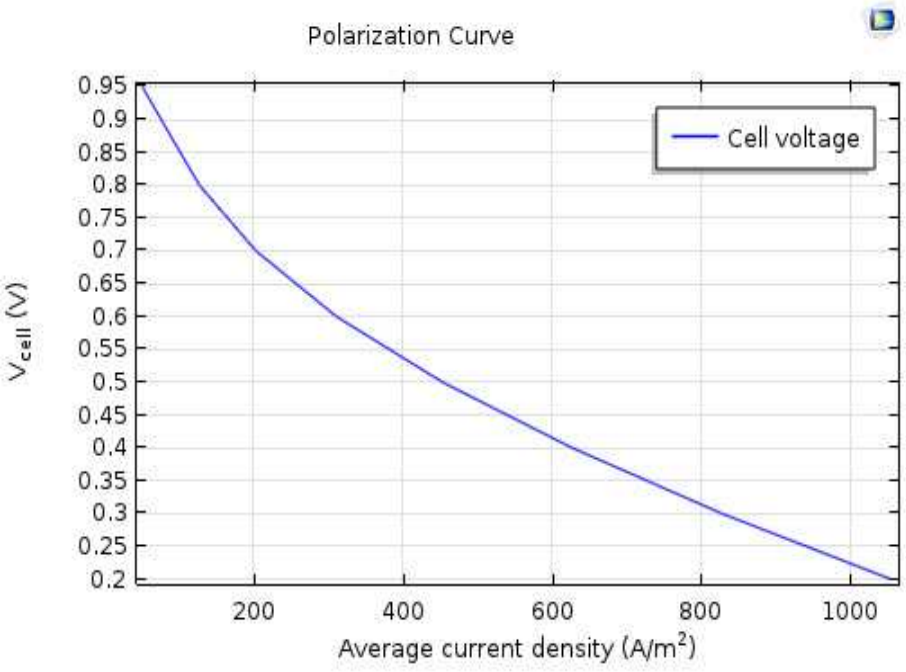

Figure 4.7: Voltage vs Current density for $SOFC_A$

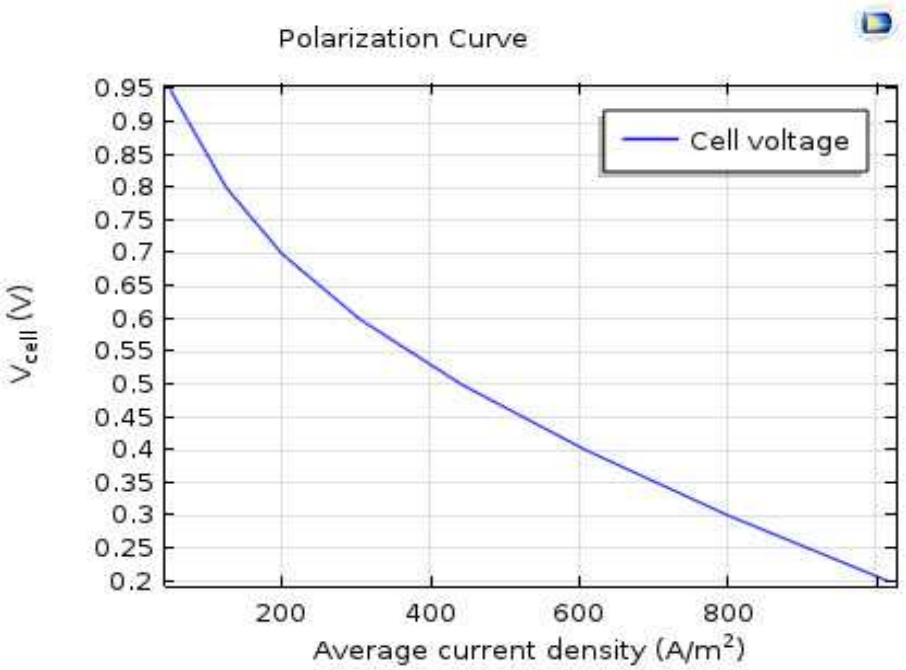

Figure 4.8: Voltage vs Current density for $SOFC_B$

4.2.3 Power Curves for Theoretical Models

Figure 4.9 and Figure 4.10 represent the variation of power density of the theoretical SOFCs with current density results obtained from equivalent COMSOL models respectively.

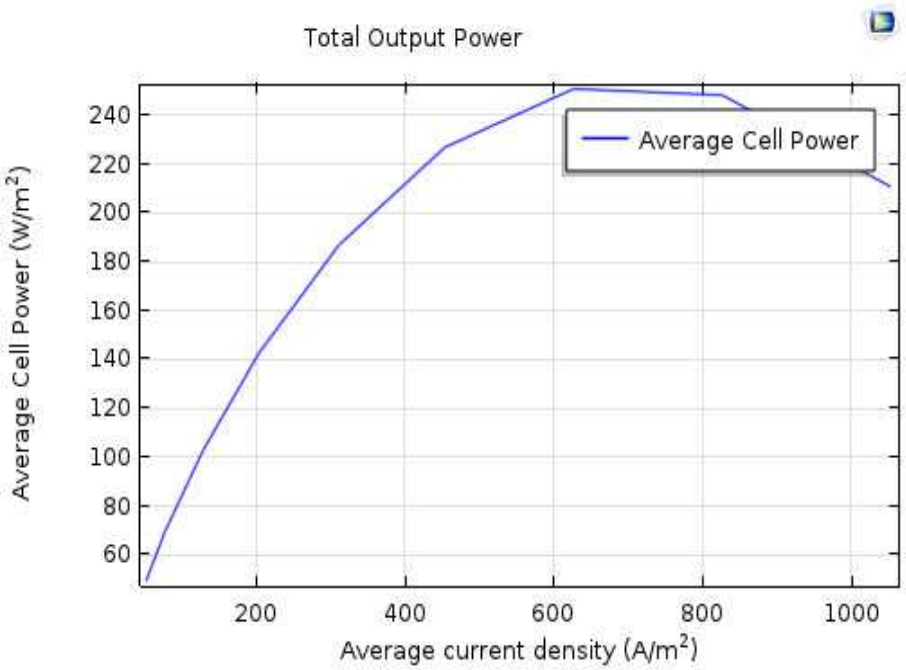

Figure 4.9: Power density vs Current density for $SOFC_A$

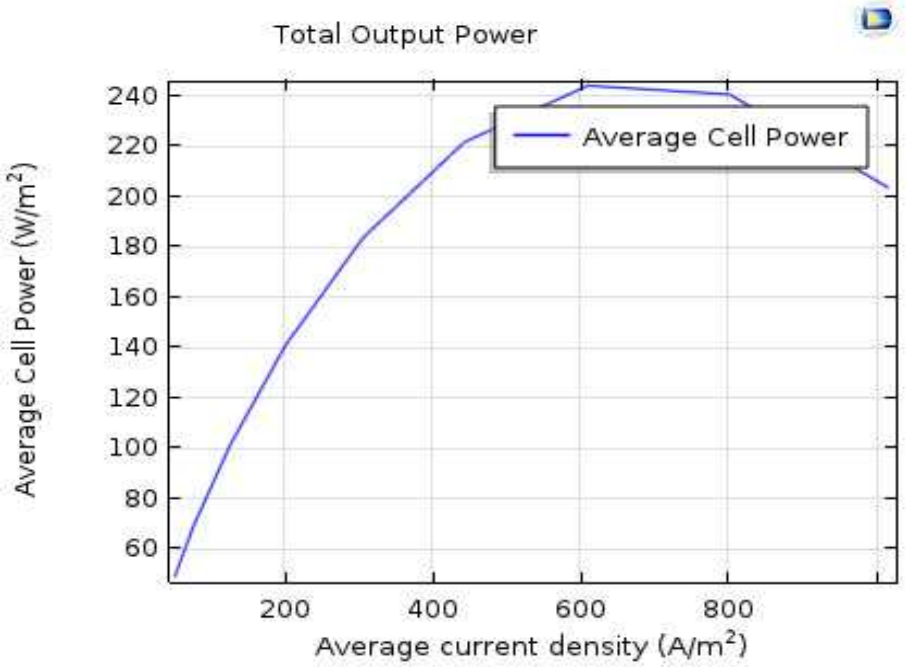

Figure 4.10: Power density vs Current density for $SOFC_B$

Chapter 5

Discussion

In this chapter, our aim is to validate the results documented in the previous chapter and evaluate the performance of the fabricated SOFCs. We start the chapter by comparing the characteristics of the fabricated SOFCs with the results obtained from the equivalent COMSOL models. Then, the characteristics of our fabricated SOFCs are compared to determine which SOFC performs better. Finally, the limitations which we faced during the thesis are discussed.

5.1 Comparison of theoretical and experimental results

In this section, we have compared the experimental results obtained from the fabricated $SOFC_A$ and $SOFC_B$ with the simulation results obtained from the equivalent COMSOL models. Figure 5.1 shows the theoretical and experimental polarization characteristics for $SOFC_A$.

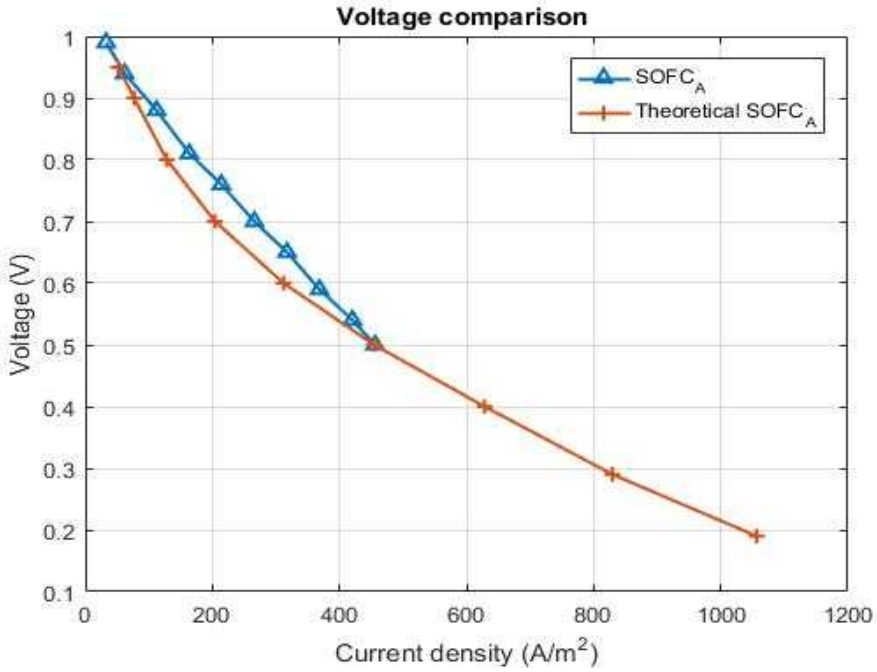

Figure 5.1: Voltage vs Current density

Figure 5.2 represents the comparison between theoretical and experimental power curves for $SOFC_A$.

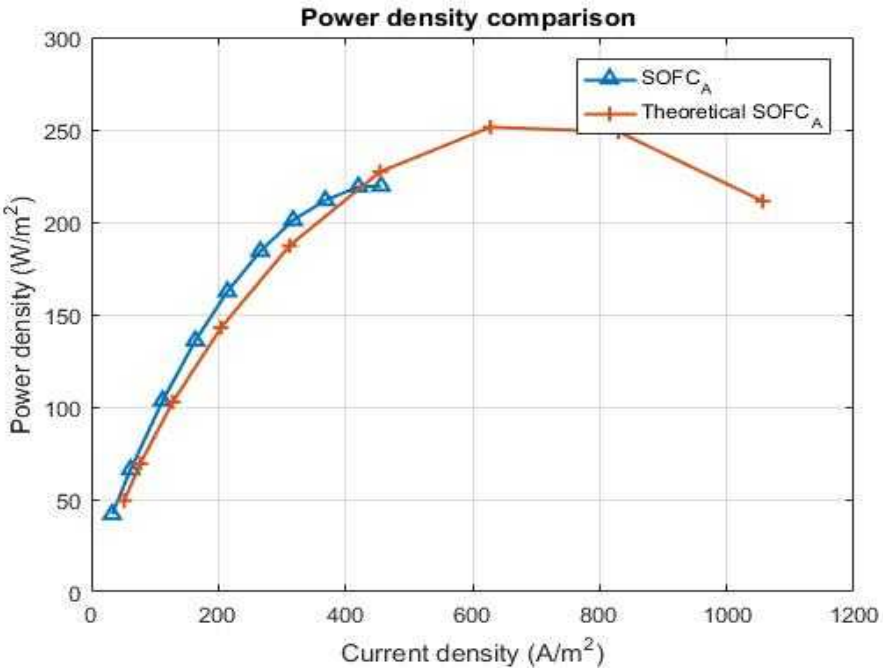

Figure 5.2: Power density vs Current density

When considering Figure 5.1, we can see that the voltage of both curves gradually decrease with the increase of the current density. Moreover, at lower values of current density, theoretical and experimental curves tend to match than for the higher values of current density. Note that, we cannot reduce the cell voltage below 450 mV, since it may damage the SOFC. Hence, we are unable to plot the experimental curves for the full range of current density values.

In Figures 5.3 and 5.4, we provide the comparison between experimental and theoretical results in relation to $SOFC_B$. Theoretical and experimental polarization curves for $SOFC_B$ is almost identical to the respective polarization curves of $SOFC_A$. However, it is observable that the theoretical and experimental power curves for $SOFC_B$ exhibits less deviation (between curves) than the corresponding power curves for $SOFC_A$.

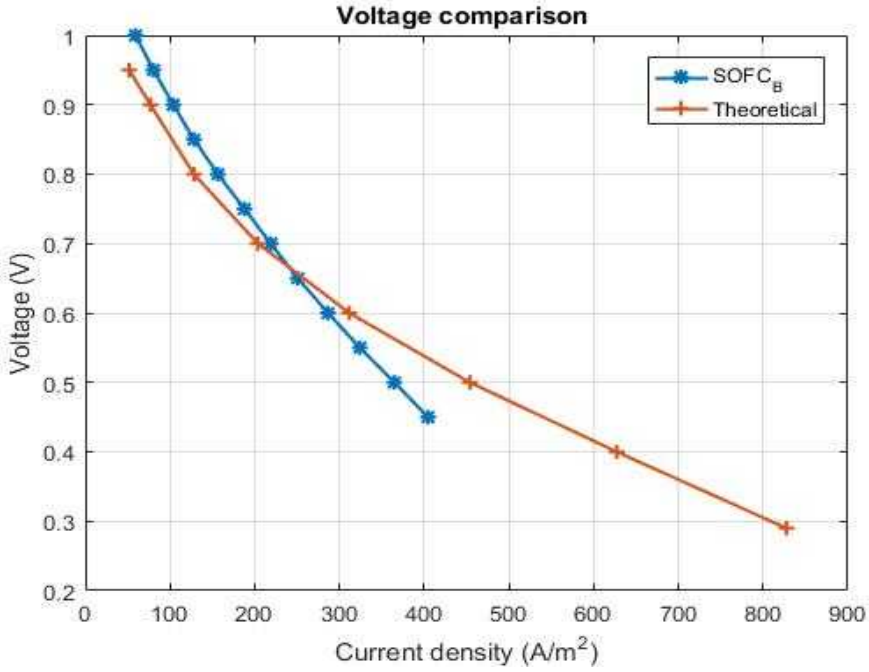

Figure 5.3: Voltage vs Current density

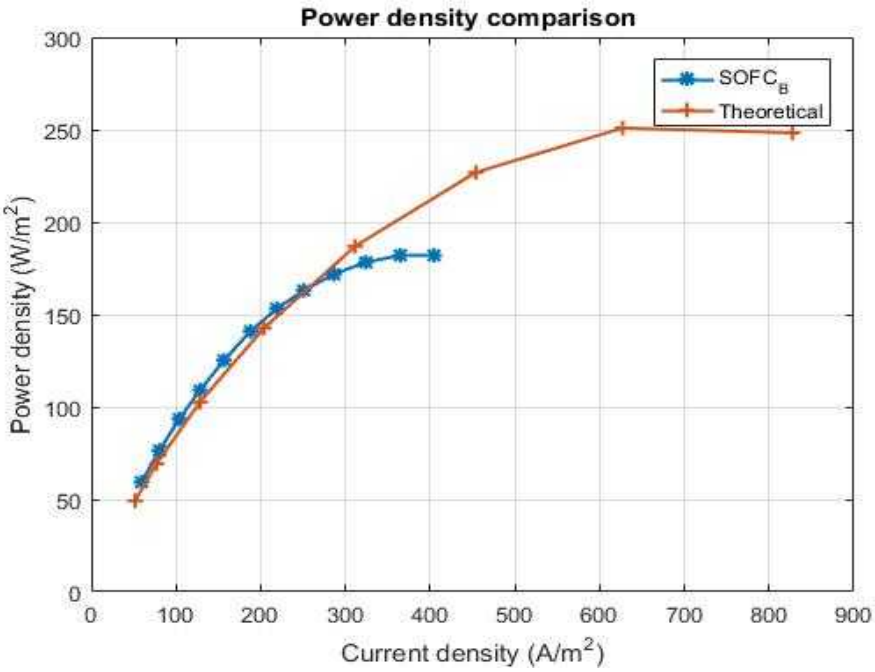

Figure 5.4: Power density vs Current density

More importantly, we can see that the experimental characteristics curves for both fabricated SOFCs resembles their corresponding theoretical characteristics. Hence, it is evident that our experimental results are valid. Furthermore, some of the possible reasons for the deviations in theoretical and experimental characteristics are discussed in Section 5.3, where we pointed out the limitations associated with our work.

5.2 Performance Comparison of $SOFC_A$ and $SOFC_B$

In this section, we compare the performance of $SOFC_A$ and $SOFC_B$. Figure 5.5 represents the comparison of polarization characteristics while Figure 5.6 represents the power characteristics of $SOFC_A$ and $SOFC_B$. According to the figures, it is evident that $SOFC_A$ has better characteristics than $SOFC_B$.

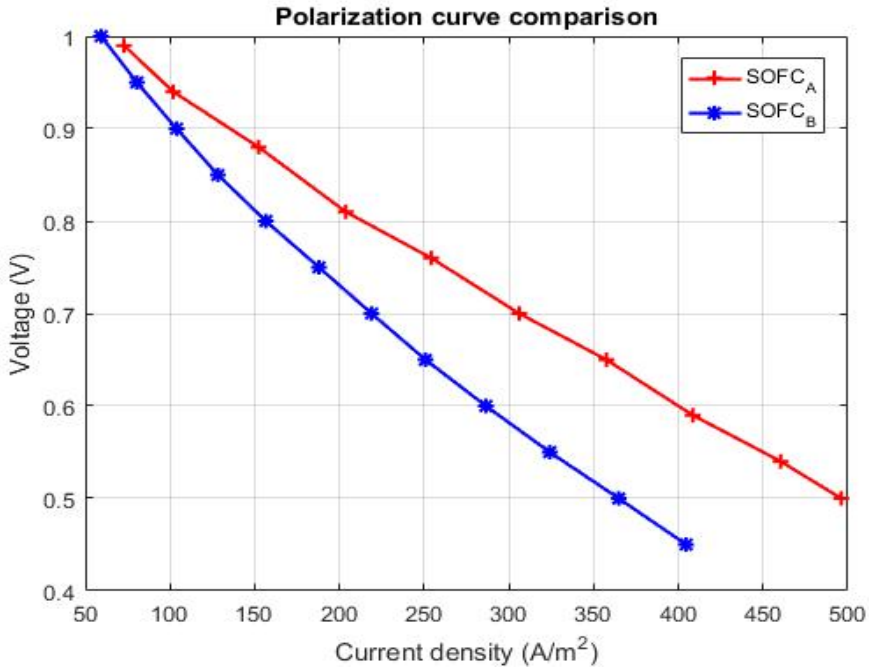

Figure 5.5: Voltage vs Current density

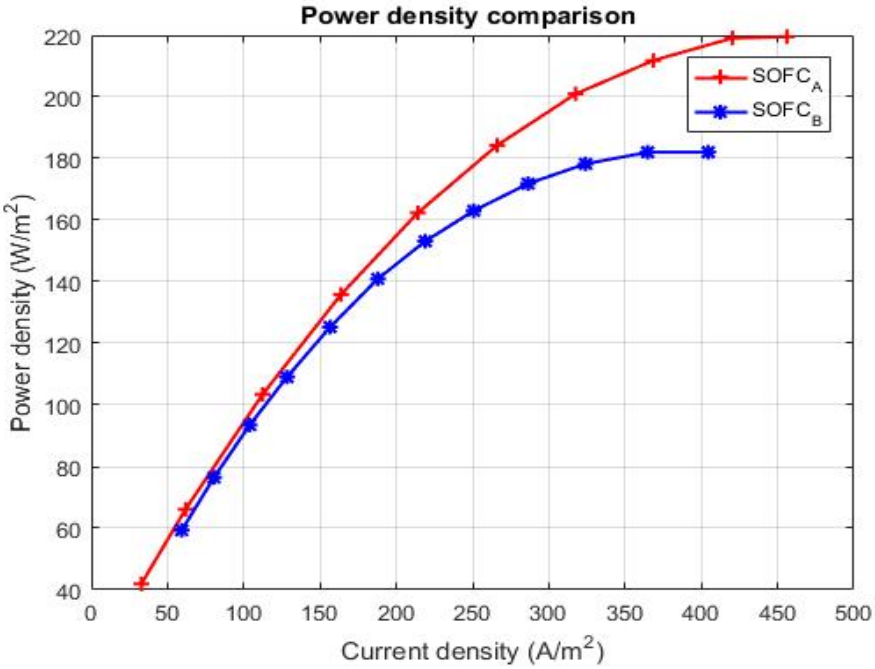

Figure 5.6: Power density vs Current density

In comparing $SOFC_A$ and $SOFC_B$, it is evident that the performance of $SOFC_A$ is better that $SOFC_B$. The reason can be determined by the composition of the anode support as given in the Table 3.1 (copied below)

Table 3.1: Comparison of chemical compositions of SOFCs (wt%)

		$SOFC_A$	$SOFC_B$	Particle Surface Area (m^2/g)	Particle Density (μm)
Porous Anode	NiO_2	60%	55%	7.23	0.63
	$3Y$	40%	50%	11	0.43
	$Polymer$	30%	40%	-	-
Active Layer	NiO_2	60%	55%	8-12	0.3-0.6
	$3Y$	40%	50%	11	0.43
	$Polymer$	30%	40%	-	-
Electrolyte	$8Y$	75%	75%	8.3	0.45
	$Polymer$	25%	25%	-	-
GDC Layer	20 GDC	46%	46%	-	-
Cathode	$LSCF$	53%	53%	-	-

In $SOFC_A$ we used 60% NiO_2 whereas in $SOFC_B$ we decreased this to 55%. The deviation of 5% will have the effect of increasing the amount of NiO_2 in the substrate and decreasing the amount of YSZ. This can affect the microstructure of the substrate and also the active surface area (number of 3-phase contact points). In a simple assessment we can conclude that by increasing the NiO_2 content by 5% will increase the porosity of the substrate towards hydrogen diffusion and thereby increasing the supply of H_2 to the active parts of the electrode where the triple phase boundaries exist. Overall this gives rise to a better cell performance.

It was outside the scope to this study to perform a full microstructural investigation on the fabricated cells, but we intend this to be a subject for the further studies. However in both cases we obtained very respectable performances from a formulation that has far from been optimized. Quoting power at the standard value of cell voltage at $0.7\,V$, for the fabricated SOFCs are tabulated in Table 5.1.

Table 5.1: Quoting power at the standard value of cell voltage at $0.7\,V$

Cell Type	Power ($mW\ cm^{-2}$)
$SOFC_A$	190
$SOFC_B$	150

5.3 Limitations in the Tape Casting Procedure

In this section, the limitations associated with this thesis are discussed. We have pointed out the limitations which we faced when fabricating the SOFCs as well as performing experiments.

When fabricating the anode and the electrolyte, we need to add 1.6 g of water for 1 g of ceramic powder. In addition, we require polymer and dispersant liquids to make the slurry. However, we do not know the exact water percentage associated with the polymer and the dispersant used for our fabrications. Therefore, the percentage of solvent added may not be exactly 1.6 g for 1 g of ceramic powder.

During the sintering process, we need to place the anode and the electrolyte in between two *setting plates* to avoid uneven surfaces. In the lab, we have only one set of plates. If the weight of these plates are high, it might not create a good ceramic and may also create cracks in the ceramic.

When fabricating the cathode using screen printing, the cathode slurry is applied on top of the sintered SOFC with a certain angle. If this angle is too high, the amount of paste passing through the screen will be low, creating a thinner cathode. Furthermore, if the angle is too low, the amount of paste passing through the screen will be high, which might lead to a cathode with an uneven surface.

It is necessary to supply gases through a channel to the middle of the anode and the cathode during experiments in such a way that the gases evenly distribute through the surface. If the gas supply is not evenly distributed through the surface, it may cause uneven voltage and current levels along the surface of the electrodes. Furthermore, we can only vary the voltage of the cell from OCV to 450 mV, since reducing the cell voltage less than 450 mV could potentially damage the SOFC. Hence, we cannot obtain the complete experimental characteristics as evident from Figure 5.2.

These limitations may have lead to the slight deviations in the theoretical and experimental characteristics.

Chapter 6

Conclusion

In this chapter, we conclude the thesis by providing a summarization on the objectives, main results and our contribution as well as introducing new research directions that have invoked as a result of our analysis.

The main objective of this thesis was to analyze the effect of electrode chemical compositions on the performance of the planar anode supported SOFCs as well as validating the experimental results with the help of equivalent theoretical models. Furthermore, we fabricated the SOFCs in such away that there is an active layer (NiO_2) in between the anode and the electrolyte as well as a barrier layer (GDC) in between the electrolyte and the cathode. Hence, the SOFCs have five layers instead of the more common 3 layer architecture. For the analytical purposes, we fabricated two SOFCs ($SOFC_A$ and $SOFC_B$) with different chemical compositions. To be exact for the $SOFC_A$, we used 60% NiO_2, 40% $3Y$ and 30% polymer for the anode whereas 75% $8Y$ and 25% polymer were used for the electrolyte. Furthermore, we used cathode ink with 53% $LSCF$ for the cathode fabrication. However, for $SOFC_B$ we used 55% NiO_2, 50% $3Y$ and 40% polymer for the anode while the chemical compositions for the electrolyte and the cathode were same as in $SOFC_A$. When fabricating the anode and the electrolyte, we used water as the solvent rather than using organic solvents which is the most common industrial standard. Hence, our fabrications are more environmentally friendlier due to the fact that we minimized the use of hazardous organic solvents.

To evaluate the performance, we obtained the polarization and power characteristics for both of the fabricated SOFCs by carrying out experiments. In order to validate the obtained experimental characteristics, two theoretical 3D COMSOL models equivalent to the fabricated SOFCs were developed. Furthermore, with the help of appropriate simulations, we obtained the theoretical polarization and power characteristics for both SOFCs. Finally, we compared the experimental characteristics of the two fabricated SOFCs with the simulation results obtained from the equivalent theoretical COMSOL models.

With the help of Figures 5.1 to 5.4, we have shown that the experimental characteristics for both fabricated SOFCs resembles their corresponding theoretical characteristics. Hence, it is evident that our experimental results are valid. According to Figure 5.5 and Figure 5.6, we can see that the $SOFC_A$ has better performance by means of both the polarization and power

characteristics than $SOFC_B$. Thus, it is evident that the chemical composition we have used for fabricating $SOFC_A$ yields better performance. Hence, it is fair to conclude that, when the percentage of NiO_2 is higher in the anode, SOFCs exhibits better performance.

Our performance data obtained on the two SOFC compositions ($SOFC_A = 190\, mW\ cm^{-2}$, $SOFC_B = 150\, mW\ cm^{-2}$, both at $0.7\, V$) are very encouraging and show that an all water based tape casting procedure can produce results that are comparable to more convention solvent based systems. In future work, we will optimise the composition to increase the power densities.

In order to fabricate the anode and the electrolyte of our SOFCs, we used water as the solvent when making the respective slurries whereas for the cathode, we used a commercial cathode ink made of organic solvents. These organic solvents are expensive and therefore it affects the total fabrication cost of a SOFC. However, if we can use water as the solvent for the cathode as we used for the anode and for the electrolyte, the cost can be reduced and the fabrication process will be much more environmentally friendlier. Therefore, investigating the possibility of using water as a solvent for cathode fabrication instead of using an organic solvent might also be an interesting extension to our work.

Bibliography

[1] "Fuel cell today - SOFC," Accessed: 28.08.2016. [Online]. Available: http://www.fuelcelltoday.com/technologies/sofc

[2] "Ceramic energy: Advances in sofc materials and manufacturing," Accessed: 02.09.2016. [Online]. Available: http://www.ceramicindustry.com/articles/86115-ceramic-energy-advances-in-sofc-materials-and-manufacturing

[3] "Tape casting material processing," Accessed: 30.08.2016. [Online]. Available: https://global.britannica.com/technology/tape-casting

[4] A. Hobby, "Printing thick film hybrids," Accessed: 07.09.2016. [Online]. Available: http://www.gwent.org/gem_thick_film.html

[5] "Scientific principles," Accessed: 03.09.2016. [Online]. Available: http://matse1.matse.illinois.edu/ceramics/prin.html

[6] J. Janesch, "Two-wire vs. four-wire resistance measurements: Which configuration makes sense for your application," Accessed: 29.08.2016. [Online]. Available: http://www.tek.com/sites/tek.com/files/media/document/resources/2Wire_4Wire%20Resistance%20Article.pdf

[7] M. Skrzypkiewicz, "Setup of a test bench and testing the single solid oxide fuel cell at various temperatures," Master's thesis, University of Iceland & the University of Akureyr, February 2009.

[8] X. Li, *Principles of Fuel Cell*. Taylor and Francis, 2006, ISBN:1-59169-022-6.

[9] S. C. Singhal, "Solid oxide fuel cells," Winter 2007, Accessed: 29.08.2016. [Online]. Available: https://www.electrochem.org/dl/interface/wtr/wtr07/wtr07_p41-44.pdf

[10] S. Chen, N. Lior, and W. Xiang, "Coal gasification integration with solid oxide fuel cell and chemical looping combustion for high-efficiency power generation with inherent {CO2} capture," *Applied Energy*, vol. 146, pp. 298 – 312, 2015. [Online]. Available: //www.sciencedirect.com/science/article/pii/S0306261915001361

[11] M. Cologna, "Advances in the production of planar and micro-tubular solid oxide fuel cells," Ph.D. dissertation, University of Trento - Italy, April 2009.

[12] "Solid oxide fuel cells for stationary, mobile, and military applications," *Solid State Ionics*, vol. 152153, pp. 405 – 410, 2002. [Online]. Available: http://www.sciencedirect.com/science/article/pii/S0167273802003491

[13] M. L. Chendong Zuo and M. Liu, *Chapter 2 - Solid Oxide Fuel Cells*. Springer Science & Business Media, 2012, pp. 7 – 36. [Online]. Available: http://www.sciencedirect.com/science/article/pii/B9780126546408500067

[14] V. A. Rojek-Wckner, A. K. Opitz, M. Brandner, J. Math, and M. Bram, "A novel ni/ceria-based anode for metal-supported solid oxide fuel cells," *Journal of Power Sources*, vol. 328, pp. 65 – 74, 2016. [Online]. Available: //www.sciencedirect.com/science/article/pii/S037877531630951X

[15] D. Rotureau, J.-P. Viricelle, C. Pijolat, N. Caillol, and M. Pijolat, "Development of a planar {SOFC} device using screen-printing technology," *Journal of the European Ceramic Society*, vol. 25, no. 12, pp. 2633 – 2636, 2005, elecroceramics {IXElecroceramics} {IX}. [Online]. Available: //www.sciencedirect.com/science/article/pii/S0955221905002736

[16] D. Stver, H. Buchkremer, and S. Uhlenbruck, "Processing and properties of the ceramic conductive multilayer device solid oxide fuel cell (sofc)," *Ceramics International*, vol. 30, no. 7, pp. 1107 – 1113, 2004, 3rd Asian Meeting on Electroceramics. [Online]. Available: //www.sciencedirect.com/science/article/pii/S0272884204000951

[17] T. Mahata, S. Nair, R. Lenka, and P. Sinha, "Fabrication of ni-ysz anode supported tubular {SOFC} through iso-pressing and co-firing route," *International Journal of Hydrogen Energy*, vol. 37, no. 4, pp. 3874 – 3882, 2012, international Conference on Renewable Energy (ICRE 2011). [Online]. Available: //www.sciencedirect.com/science/article/pii/S0360319911011049

[18] K.-J. Kim, S.-W. Choi, M.-Y. Kim, M.-S. Lee, Y.-S. Kim, and H.-S. Kim, "Fabrication characteristics of {SOFC} single cell with thin {LSGM} electrolyte via tape-casting and co-sintering," *Journal of Industrial and Engineering Chemistry*, vol. 42, pp. 69 – 74, 2016. [Online]. Available: //www.sciencedirect.com/science/article/pii/S1226086X16302349

[19] J. F. Beltran-Lopez, M. A. Laguna-Bercero, J. Gurauskis, and J. I. Peña, "Fabrication and characterization of graded anodes for anode-supported solid oxide fuel cells by tape casting and lamination," *Electrocatalysis*, vol. 5, no. 3, pp. 273–278, 2014. [Online]. Available: http://dx.doi.org/10.1007/s12678-014-0193-2

[20] T. V. V. S. Lakshmi, P. Geethanjali, and P. S. Krishna, "Mathematical modelling of solid oxide fuel cell using matlab/simulink," in *Emerging Research Areas and 2013 International Conference on Microelectronics, Communications and Renewable Energy (AICERA/ICMiCR), 2013 Annual International Conference on*, June 2013, pp. 1–5.

[21] A. Gebregergis, P. Pillay, D. Bhattacharyya, and R. Rengaswemy, "Solid oxide fuel cell modeling," *IEEE Transactions on Industrial Electronics*, vol. 56, no. 1, pp. 139–148, Jan 2009.

[22] M. Andersson, "Sofc modeling considering mass and heat transfer, fluid flow with internal reforming reactions," Master's thesis, LUND University, January 2009.

[23] H. Paradis, "CFD simulations of transport processes including chemical reactions in sofcs," Master's thesis, LUND University, 2009.

[24] J. W. Dennis, "Tape casting advanced materials," Accessed: 30.08.2016. [Online]. Available: http://www.ceramicindustry.com/articles/88246-tape-casting-advanced-materials

[25] "Solid oxide fuel cell," Accessed: 29.08.2016. [Online]. Available: https://en.wikipedia.org/wiki/Solid_oxide_fuel_cell

[26] L. C. D. Jonghe and M. N. Rahaman, *Chapter 4 - 4.1 Sintering of Ceramics*. Oxford: Academic Press, 2003, pp. 187 – 264. [Online]. Available: http://www.sciencedirect.com/science/article/pii/B9780126546408500067

[27] "Kelvin (4-wire) resistance measurement," Accessed: 29.08.2016. [Online]. Available: http://www.allaboutcircuits.com/textbook/direct-current/chpt-8/kelvin-resistance-measurement/

[28] "Maxwell-stefan diffusion and convection," Accessed: 28.12.2016. [Online]. Available: https://lost-contact.mit.edu/afs/pdc.kth.se/roots/ilse/v0.7/pdc/vol/comsol/3.2/amd64_fc3/doc/chem/wwhelp/wwhimpl/common/html/wwhelp.htm?context=chem&file=chem31_ug_mass-4.html

[29] "Comsol multiphysics cyclopedia," Accessed: 10.12.2016. [Online]. Available: https://www.comsol.no/multiphysics

[30] H. C. Brinkman, "A calculation of the viscous force exerted by a flowing fluid on a dense swarm of particles," *Flow, Turbulence and Combustion*, vol. 1, no. 1, p. 27, 1949. [Online]. Available: http://dx.doi.org/10.1007/BF02120313

[31] M. Kobera, "Brinkman equations as a model for flows in porous media," in *WDS'08 Proceedings of Contributed Papers, Part III*, 2008, pp. 38–43.

[32] D. Noren and M. Hoffman, "Clarifying the butlervolmer equation and related approximations for calculating activation losses in solid oxide fuel cell models," *Journal of Power Sources*, vol. 152, pp. 175 – 181, 2005. [Online]. Available: //www.sciencedirect.com/science/article/pii/S037877530500563X

[33] K. S. T. Hosoia, T. Yonekuraa and K. Sasaki, "Exchange current density of sofc electrodes: Theoretical relations and partial pressure dependencies rate-determined by electrochemical reactions," *Journal of Electrochemical Society*, vol. 162, pp. 136 – 152, 2015. [Online]. Available: http://jes.ecsdl.org/content/162/1/F136.full

Appendix A

In Appendix A, we have described the processes along with the respective governing equations associated with the modelling of theoretical SOFC model using COMSOL Multiphysics software.

When simulating the developed COMSOL models, the equations for momentum, charge balances and mass transport are solved simultaneously. The main processes associated with the functionality of the model are stated below.

- Multicomponent transport
  - Mass balances in gas phase in gas channels and porous electrodes (Maxwell-Stefan Diffusion and Convection)
- Gas diffusion
  - Flow distribution in gas channels (Navier-Stokes)
  - Flow in the porous GDEs (Brinkman equations)
- Charge Balances (Ionic and Electronic)
  - Ion charge balance (Ohm's law)
  - Electronic charge balance (Ohm's law)
  - Butler-Volmer charge transfer kinetics

In the following sections, aforementioned processes and the related governing equations are mentioned.

A.1 Multicomponent Transport in Model

Although SOFCs support fuel flexibility, we used pure H_2 and air as fuels for this model. As the anode fuels, combination of H_2 and water vapor (humidified H_2O) are used. Furthermore, in the cathode, we used a combination of air, water vapor and N_2 as the cathode fuel.

When considering the transport of fluid, we have included both diffusion (the distribution of chemical species uniformly in space with time) and convection (the bulk motion of fluid)

of the fluid. For each electrode flow compartment (anode and cathode flow channels), the material transport is modeled by the Maxwell-Stefan's diffusion and convection equations [28]. The base of the Maxwell-Stefan diffusion and convection equation is,

$$\frac{\partial \rho \omega_i}{\partial t} + \nabla.(j_i + \rho \omega_i u) = R_i$$

where ρ denotes the density, ω_i the mass fraction, j_i is the molecular mass flux and R_i is the reaction rate of the i^{th} species, u is the velocity.

The boundary at the walls (the interfaces between the porous electrodes and the gas flow channels) of the gas channels and the electrodes are considered as zero mass flux (insulation condition). We have specified the inlet conditions (as given in Table 3.2) while considering the outlet conditions as convective flux. This means that the component transport is perpendicular to the boundary. Furthermore, it is assumed that there is continuity in all the transport compositions [29]. In our model, we have used the concentrated species interface to solve the above equations.

A.2 Gas Diffusion

In order to define the velocity field and the pressure in gas channels, we used a free and porous media flow interface. Gas flows in open channels are modelled by using the weakly compressible Navier-Stokes equation [29] as given below.

$$\rho(\frac{\partial u}{\partial t} + u.\nabla u) = -\nabla p + \nabla(\mu(\nabla u) + (\nabla u)^T) - \frac{2}{3}\mu(\nabla u)I) + F$$

where u is the fluid velocity, p is the fluid pressure, ρ is the fluid density, and μ is the fluid dynamic viscosity. This equation is constructed by combining several independent parameters. Those are

- $\rho(\frac{\partial u}{\partial t} + u.\nabla u)$: Inertial forces of the system.
- ∇p : Force created by pressure of the fluid.
- $\nabla(\mu(\nabla u) + (\nabla u)^T) - \frac{2}{3}\mu(\nabla u)I)$: Viscous forces of the system.
- F : The external forces applied to the fluid.

The flow velocities in the porous GDEs are enforced with the help of the Brinkman equations [30] [31]. The Brinkman equation is given by,

$$\nabla p = -\frac{\mu}{k}v + \mu_e \nabla^2(v)$$

where v is fluid velocity, μ is fluid viscosity, μ_e is the effective viscosity parameter.

The momentum equations are used to define the boundary conditions of the inlet channels (H_2 and air) while the outlet pressure is made equal to 1 atm.

A.3 Charge Balances (Ionic and Electronic)

A secondary current distribution interface is used to determine the ionic and electronic charge balances of the electrolyte. This includes the two GDEs as well as the anode and the cathode current feeders. We have assumed that the charge transfer current density can be described by using the Butler-Volmer charge transfer kinetics [32] [33]. Furthermore, assuming that the first electron transfer in the anode as the rate determining reaction, the equation for the charge transfer kinetics can be written as,

$$i_{a,c_t} = i_{0,a}((\frac{c_{h2}}{c_{h2,ref}})exp(\frac{0.5F}{RT}\eta) - (\frac{c_{h2o}}{c_{h20,ref}})exp(\frac{-1.5F}{RT}\eta))$$

where $i_{0,a}$ is the anode exchange current density, c_{h2} is the molar concentration of H_2, c_{h_2o} is the molar concentration of H_2O, c_t is the total concentration of species, $c_{h2,ref}$ and $c_{h2o,ref}$ is the reference molar concentrations, F is the Faraday's constant, R is the gas constant, T is the temperature and η is the overvoltage. All values are in SI units.

The overvoltage is defined by,

$$\eta = \phi_{electronic} - \phi_{ionic} - \Delta\phi_{eq}$$

where $\Delta\phi_{eq}$ is the equilibrium potential difference.

The cathode charge transfer kinetics is given by,

$$i_{c,c_t} = i_{0,c}(exp(\frac{3.5F}{RT}\eta) - x_{o2}(\frac{c_t}{c_{02,ref}})exp(\frac{-0.5F}{RT}\eta))$$

where $i_{0,c}$ is the cathode exchange current density and x_{o2} is the molar fraction of O_2
We used the anode inlet voltage as a fixed reference voltage which is equal to zero. The cathode inlet voltage (V_{cell}) is given by,

$$V_{cell} = \Delta\phi_{eq,c} - \Delta\phi_{eq,a} - V_{pol}$$

where V_{pol} is the polarization voltage.

For the model, we used $\Delta\phi_{eq,c} = 1\ V$, $\Delta\phi_{eq,a} = 0\ V$ and $0.05\ V$ ¡ V_{pol} ¡ $0.8\ V$. We have applied the insulating boundary conditions for all the external boundaries for the ionic charge balance equations of the model.

Appendix B

In Appendix B, the step by step procedure associated with modelling the equivalent SOFC models is described with the help of interface screenshots captured from the COMSOL Multiphysics software.

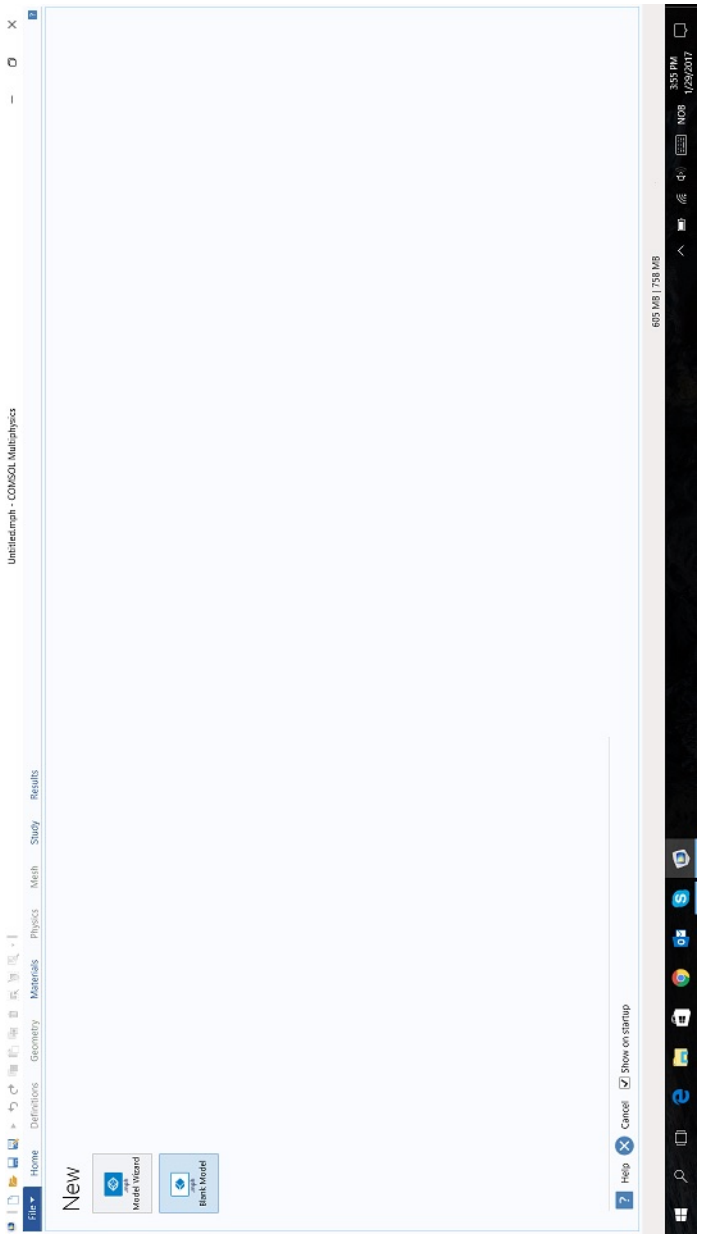

First, the model wizard in COMSOL Multiphysics software is selected.

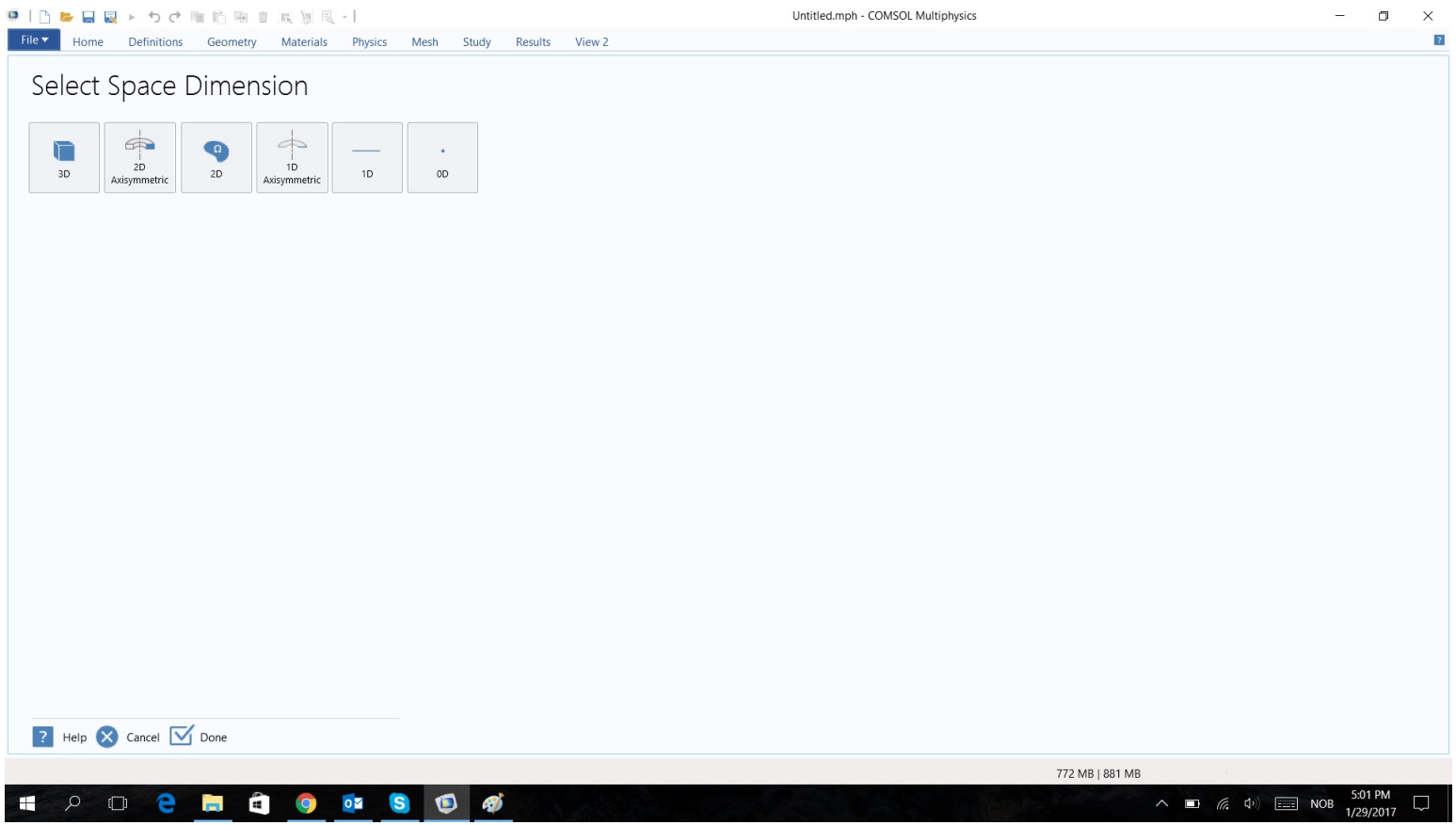

We have selected 3D as the space dimension, given that we are interested in modelling a 3D model.

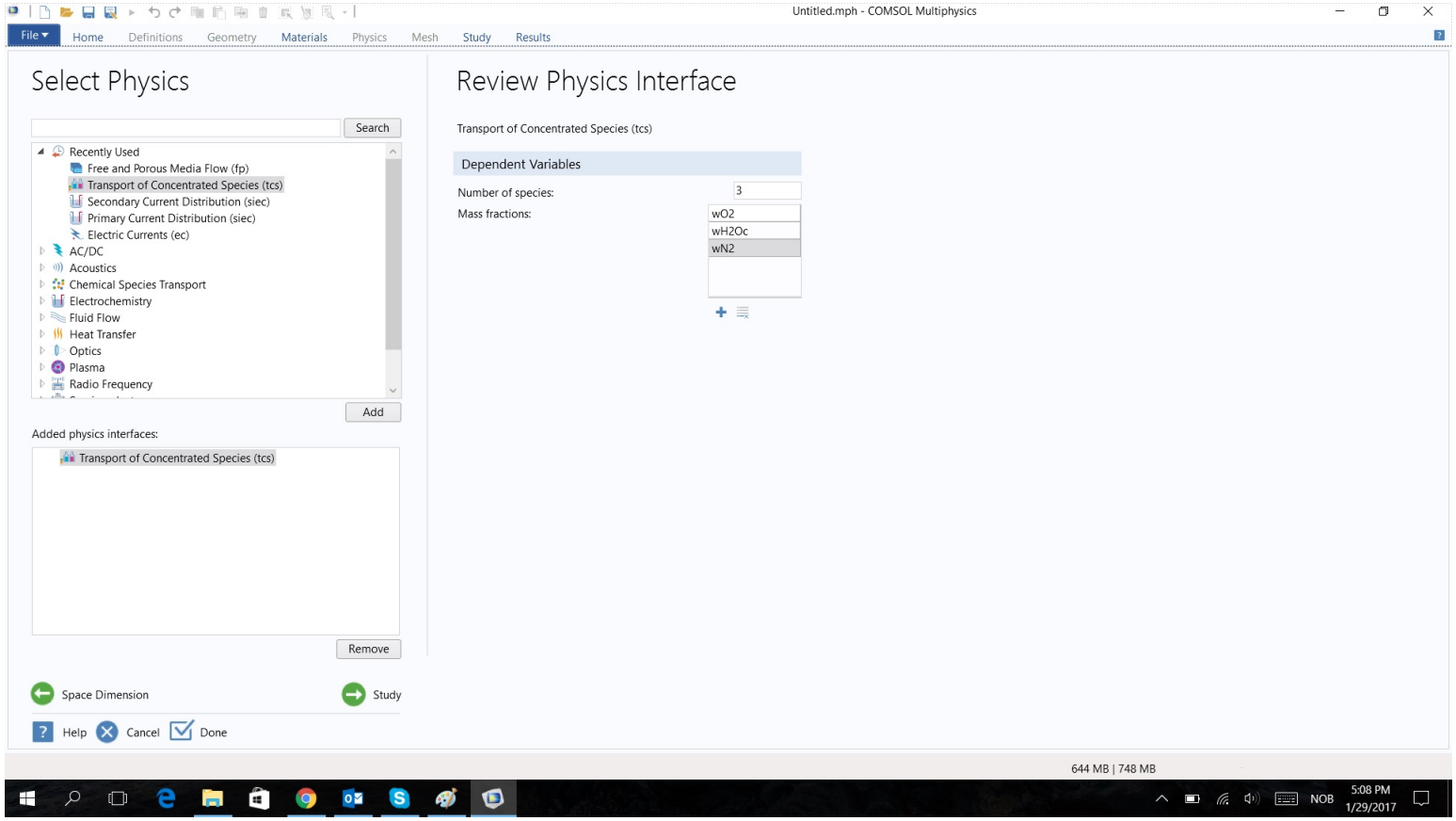

Next step is to select the physics interfaces for the model. We have selected *transport concentration of species* for both the anode and the cathode to define the mass fractions of the electrodes.

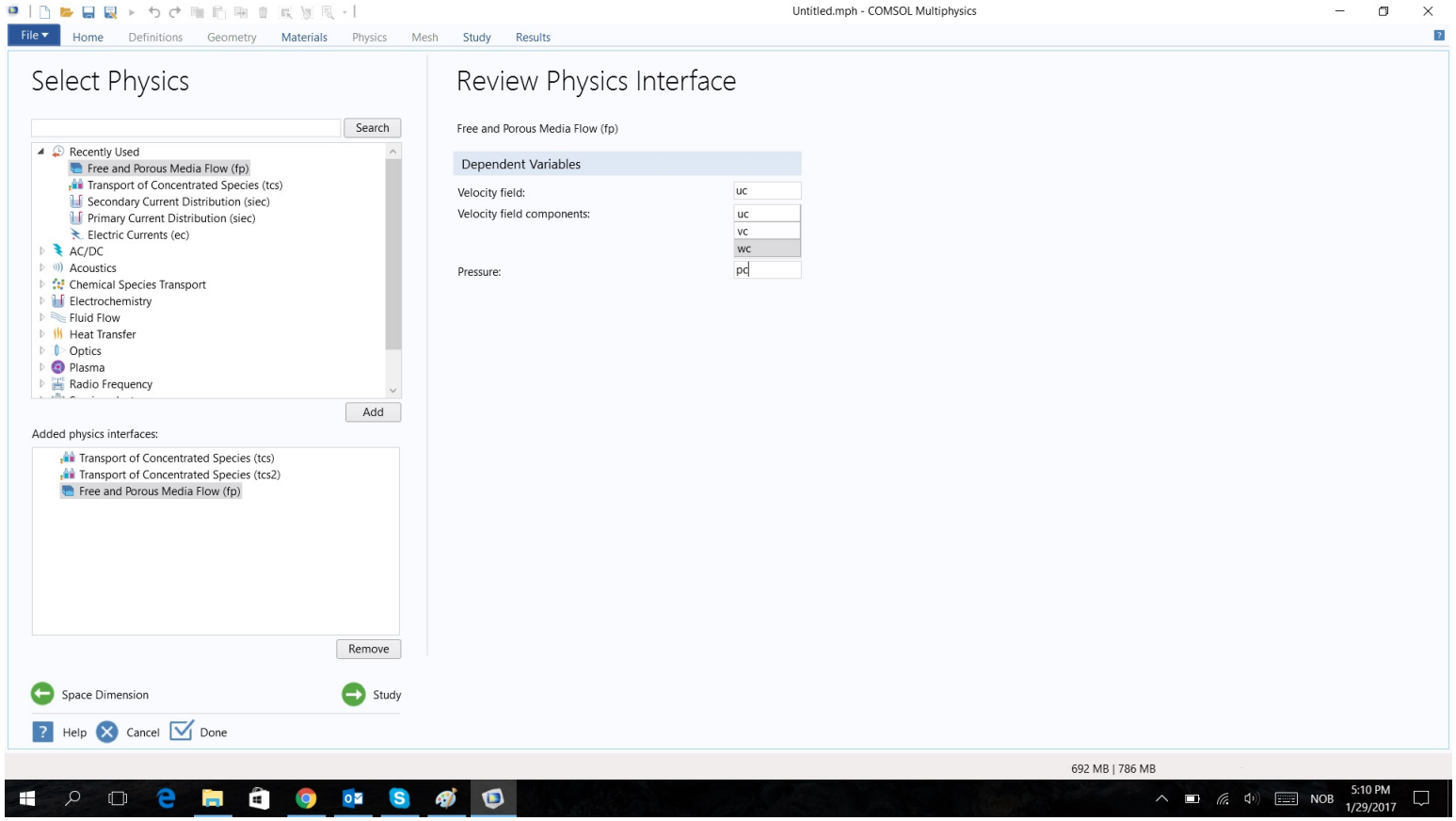

In order to define the parameters for the gas flow, we have selected the *free and porous media flow*. Pressure and the velocity components are defined for both the anode and for the cathode.

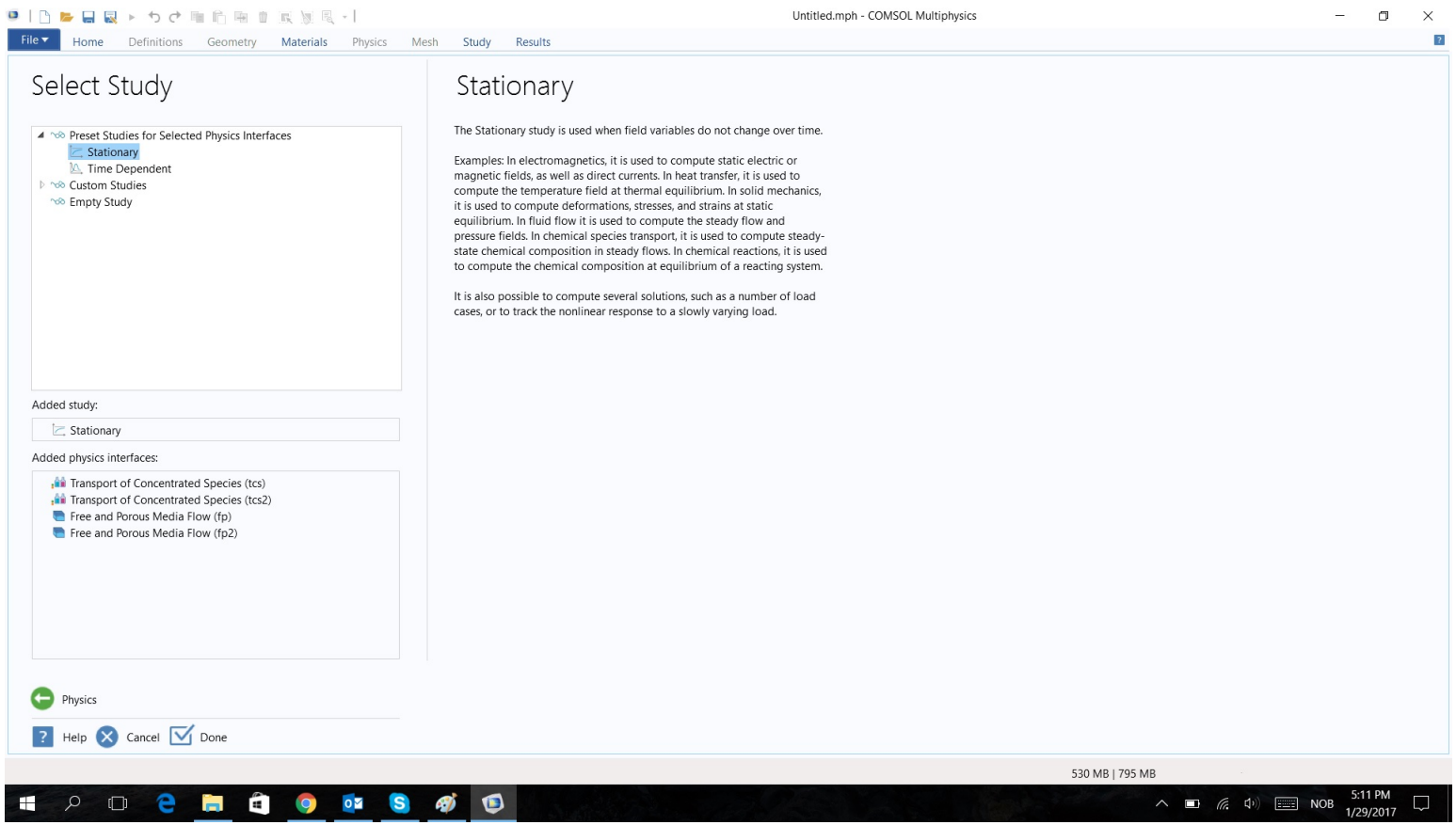

We assume that the parameters are time independent, hence we have used *stationary study* for the model.

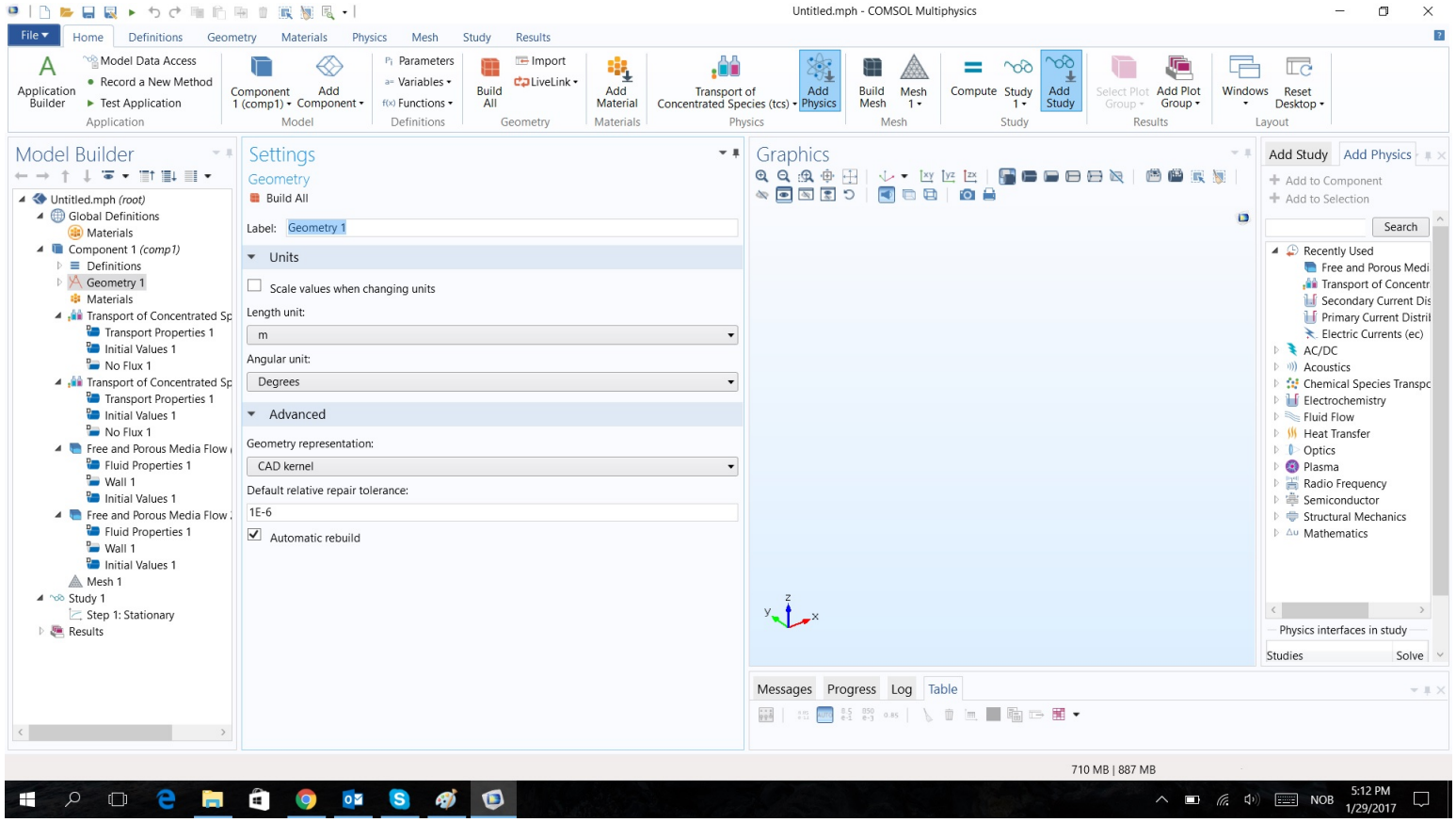

The graphic window after setting all the physics related to the model.

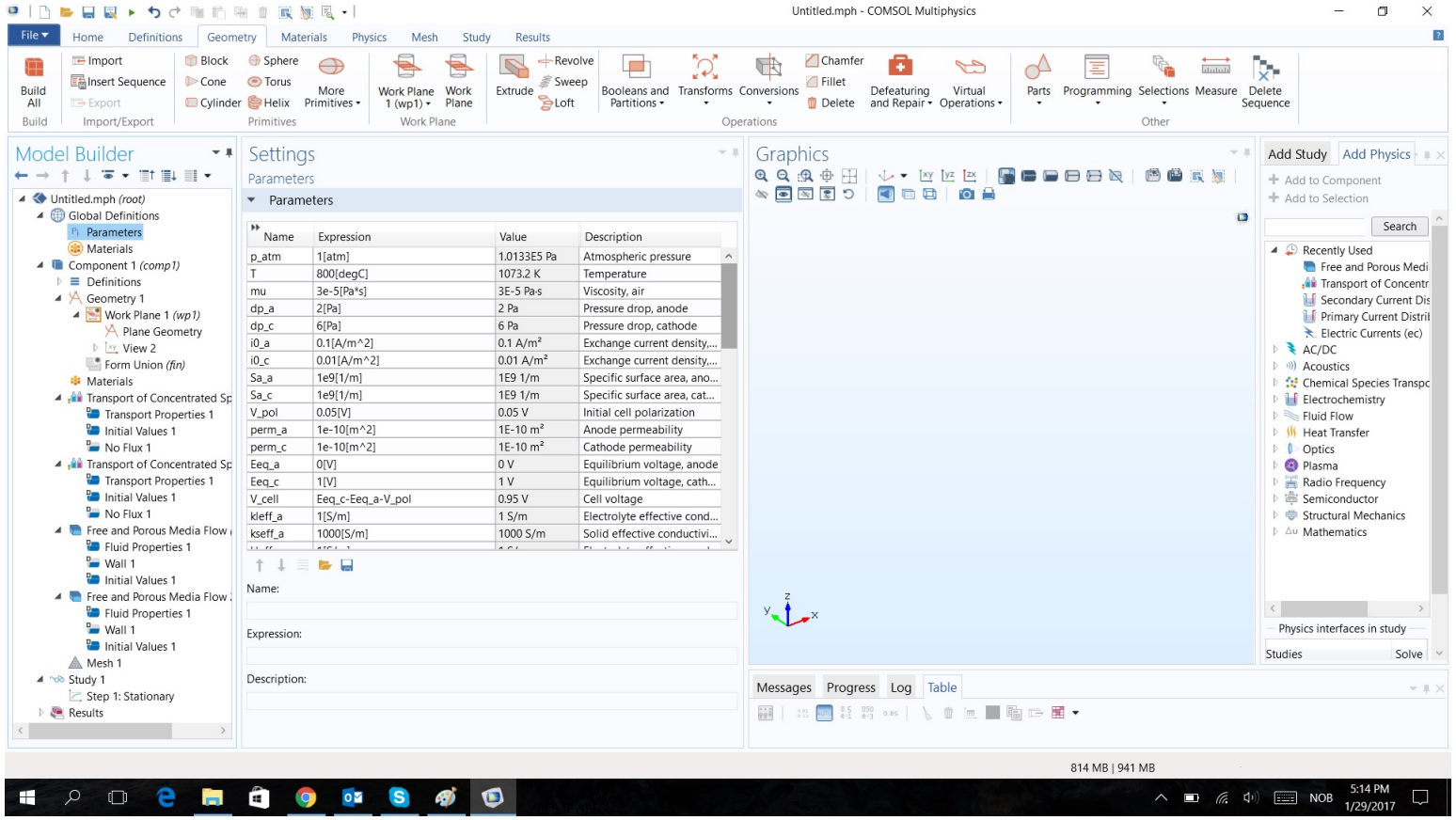

From this window, we need to setup the parameters for the model based on the parameters of the fabricated SOFCs.

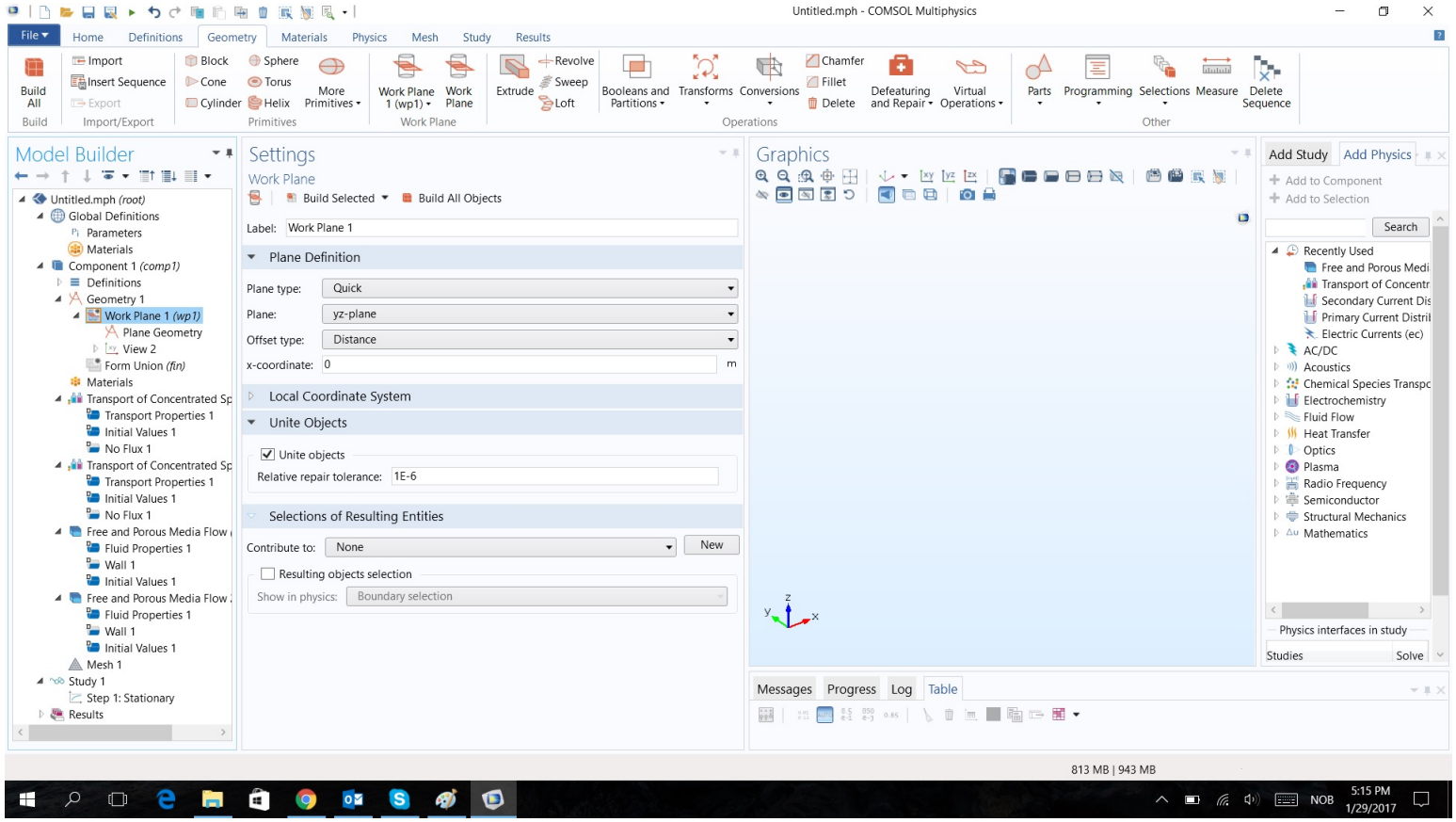

We have selected the $y-z$ *plane* as the working plane for our 2D model.

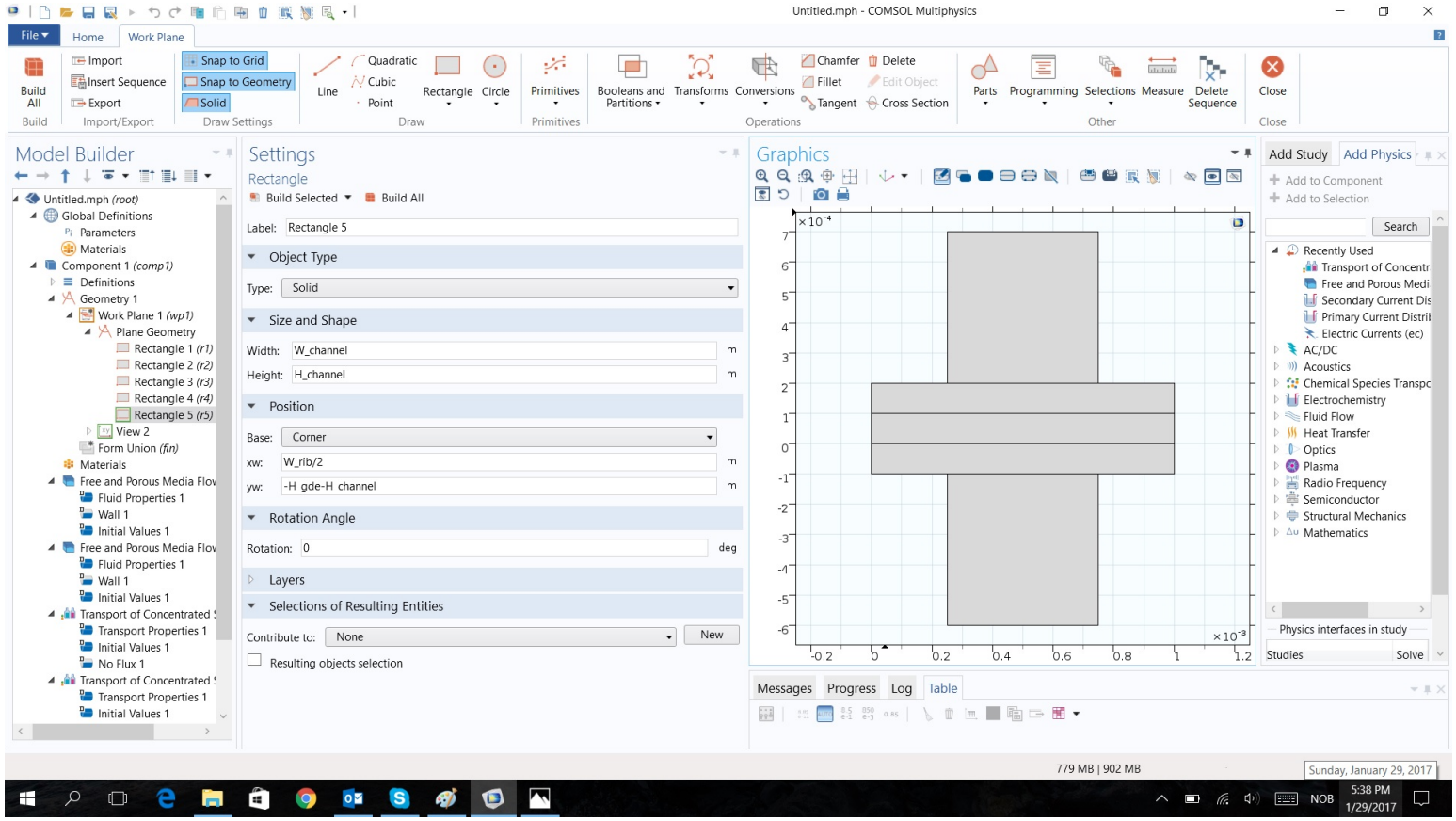

We constructed the 2D model using rectangular shapes while defining the width, thickness and the position of each layer.

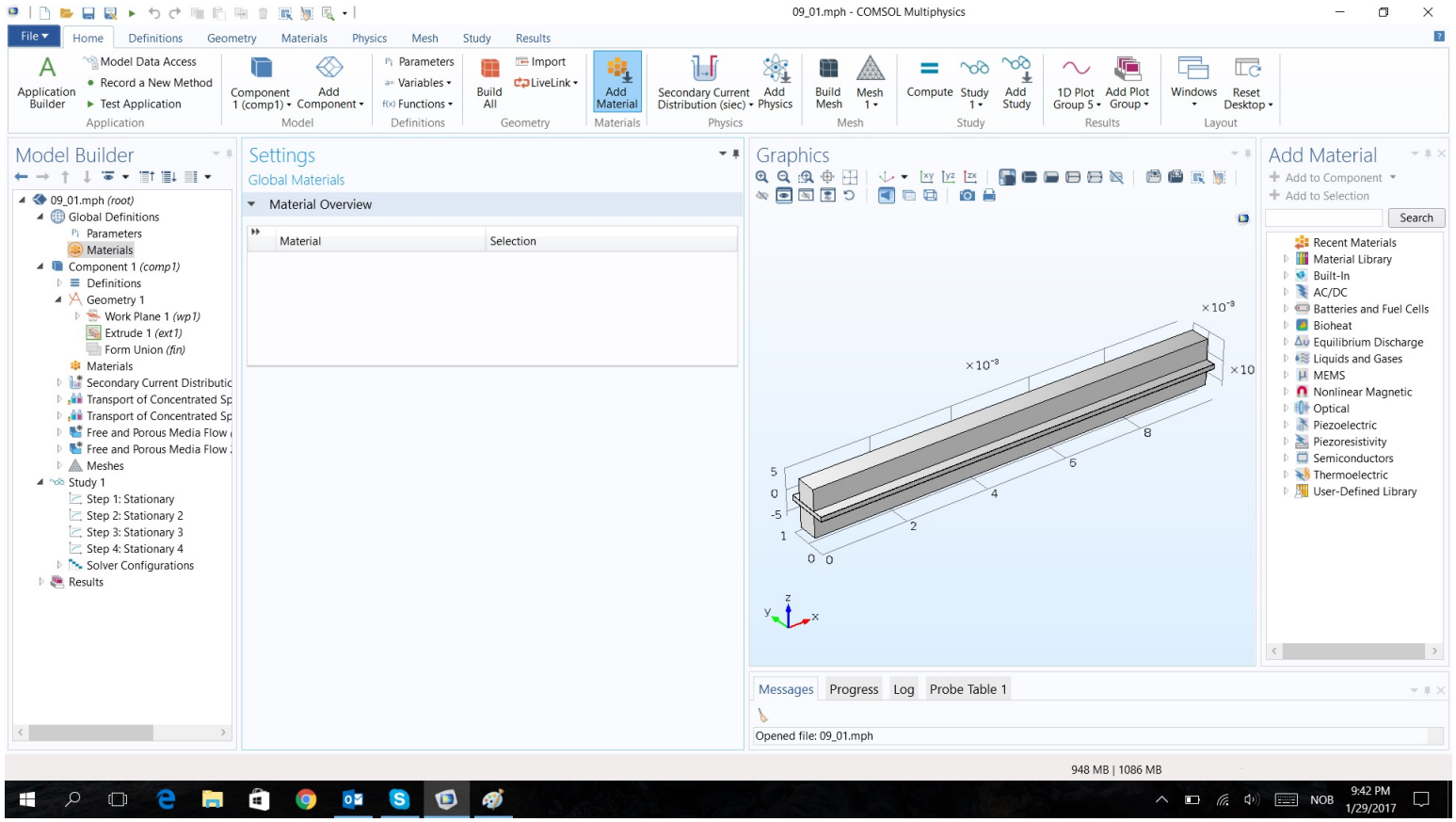

In order to obtain the 3D model, we use *extrude function* in geometry tool bar. Then, we have to set the boundary and wall conditions for the model. For each component of the model, we have to set the parameters names which we listed in the beginning.

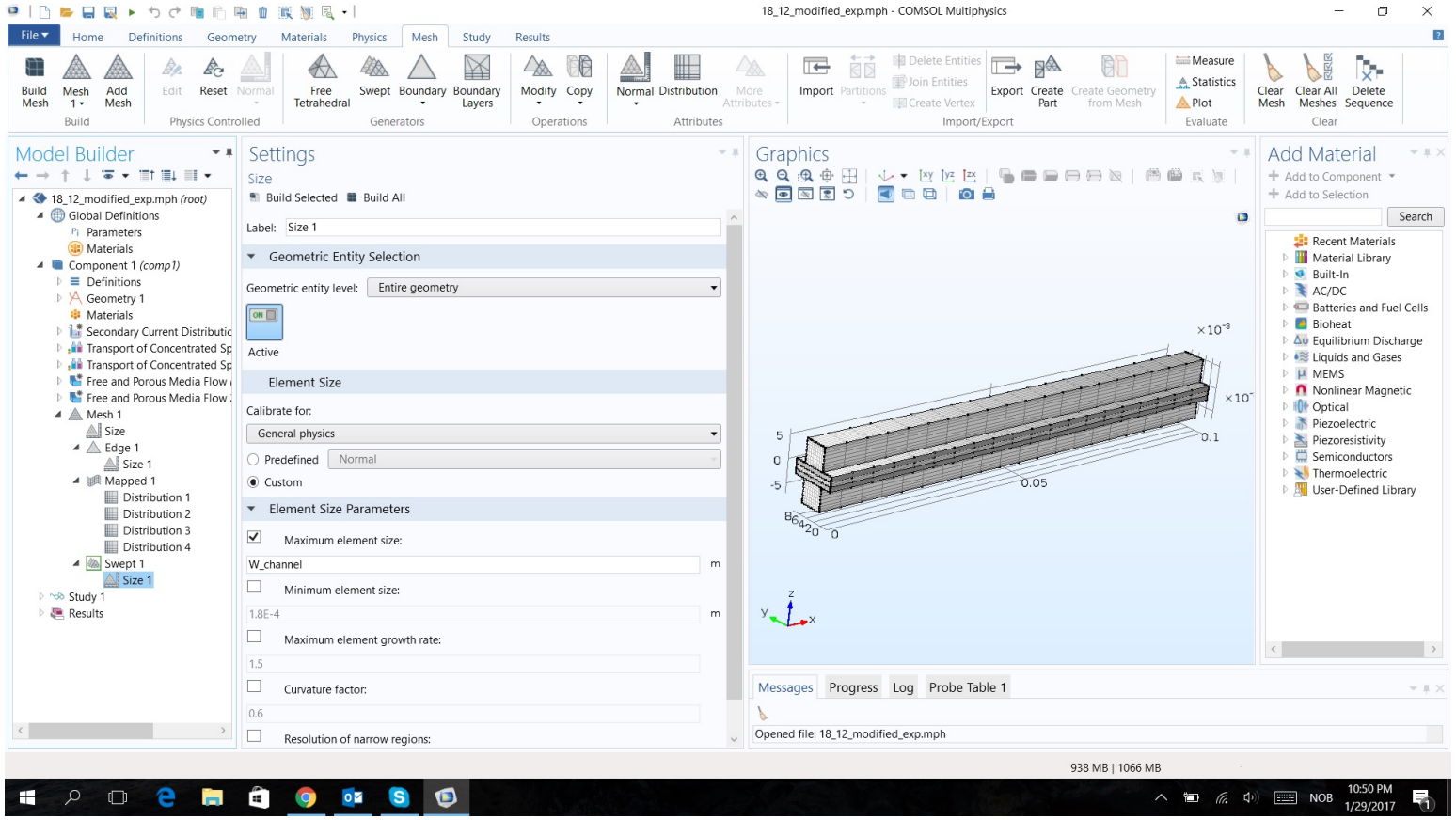

Next step is to create the mesh. Finite element method was used to discritize the model into small geographical shapes.

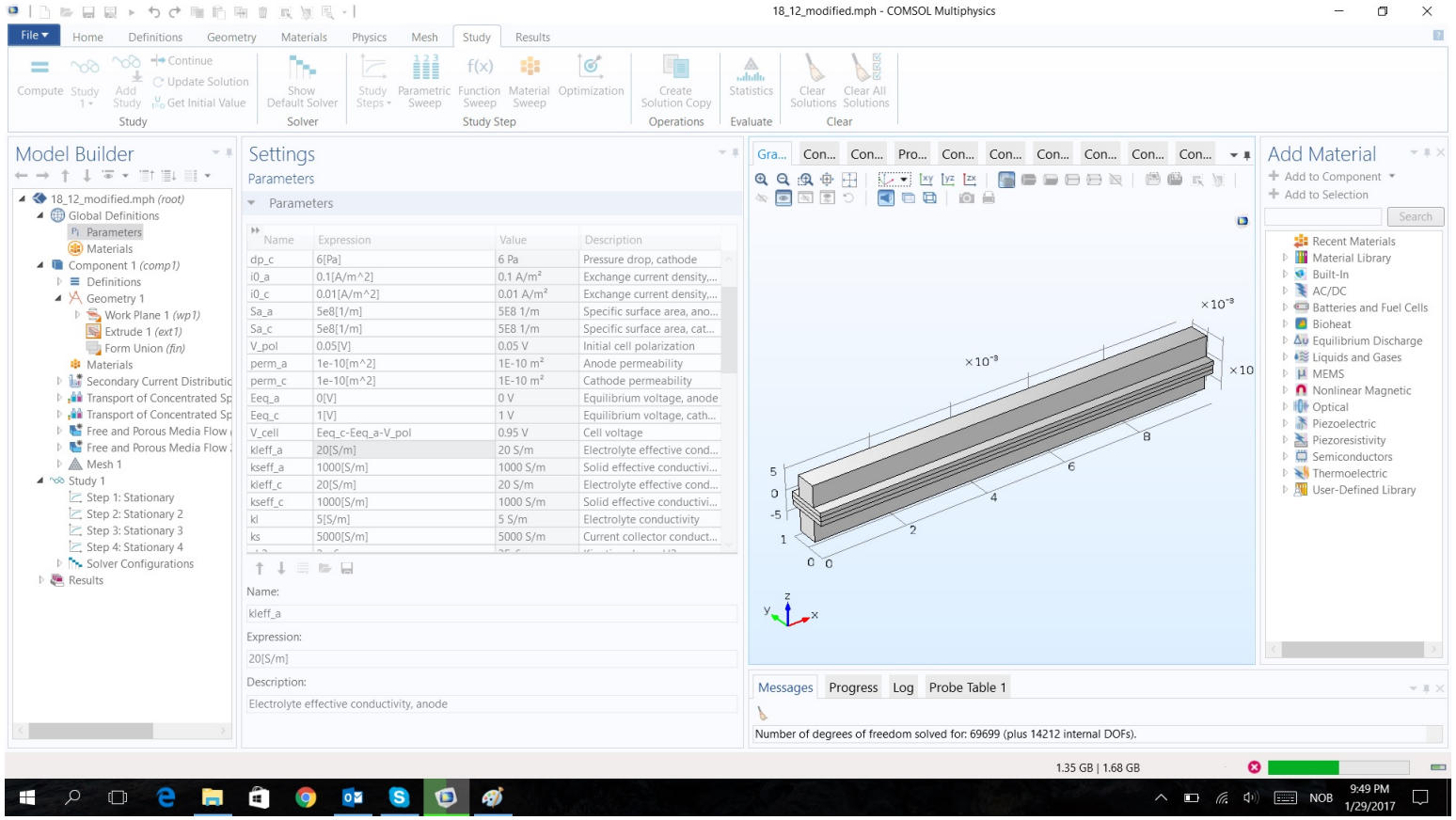

In order to obtain the simulation results, we need to run the simulation by using *compute* button in the *study* tool bar.

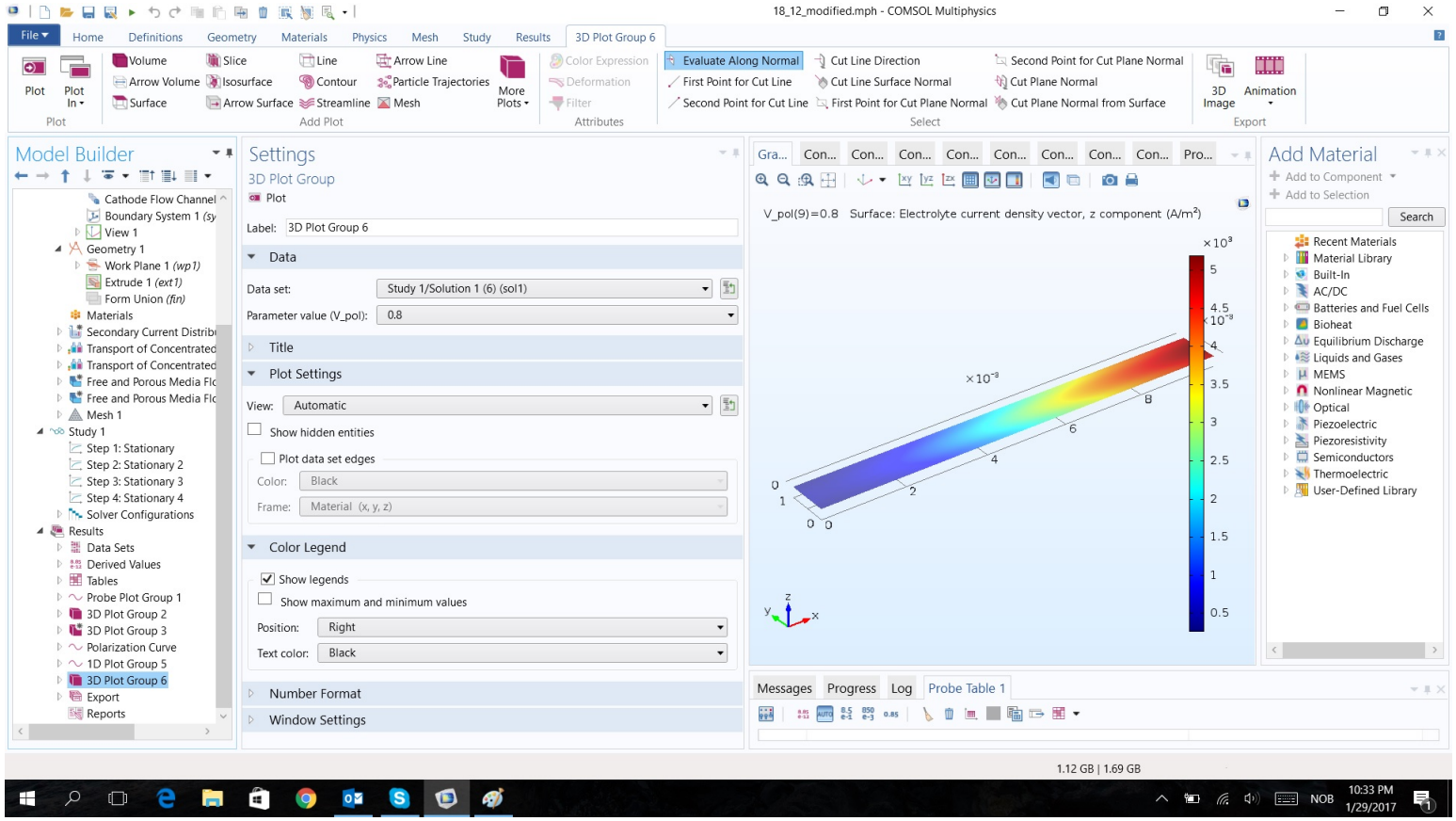

The simulation results obtained for current density distribution. Note that, after simulating the model, we need to specify which characteristics are needed to be plotted from the obtained simulation results.